

New Arylthioindoles and Related Bioisosteres at the Sulfur Bridging Group. 4. Synthesis, Tubulin Polymerization, Cell Growth Inhibition, and Molecular Modeling Studies

Giuseppe La Regina,[†] Taradas Sarkar,[§] Ruoli Bai,[§] Michael C. Edler,[§] Roberto Saletti,[‡] Antonio Coluccia,[‡] Francesco Piscitelli,^{†,♦} Lara Minelli,[†] Valerio Gatti,[†] Carmela Mazzocchi,^{†,×} Vanessa Palermo,[#] Cristina Mazzoni,[#] Claudio Falcone,[#] Anna Ivana Scovassi,[⊥] Vincenzo Giansanti,[⊥] Pietro Campiglia,[▽] Amalia Porta,[○] Bruno Maresca,[○] Ernest Hamel,[§] Andrea Brancale,[‡] Ettore Novellino,^{||} and Romano Silvestri^{*,†}

[†]Istituto Pasteur—Fondazione Cenci Bolognietti, Dipartimento di Chimica e Tecnologie del Farmaco, Sapienza Università di Roma, Piazzale Aldo Moro 5, I-00185 Roma, Italy, [‡]Welsh School of Pharmacy, Cardiff University, King Edward VII Avenue, Cardiff CF10 3NB, U.K., [§]Toxicology and Pharmacology Branch, Developmental Therapeutics Program, Division of Cancer Treatment and Diagnosis, National Cancer Institute at Frederick, National Institutes of Health, Frederick, Maryland 21702, ^{||}Dipartimento di Chimica Farmaceutica e Tossicologica, Università di Napoli Federico II, Via Domenico Montesano 49, I-80131, Napoli, Italy, [⊥]Istituto di Genetica Molecolare—Consiglio Nazionale delle Ricerche, Via Abbiategrasso 207, I-27100 Pavia, Italy, [#]Dipartimento di Biologia Cellulare e dello Sviluppo, Sapienza Università di Roma, Piazzale Aldo Moro 5, I-00185 Roma, Italy, [▽]Università di Salerno, Dipartimento di Scienze Farmaceutiche, Sezione Chimico-Tecnologica, Via Ponte don Melillo, I-84084 Fisciano, Salerno, Italy, and [○]Università di Salerno, Dipartimento di Scienze Farmaceutiche, Sezione Biomedica, Via Ponte don Melillo, I-84084 Fisciano, Salerno, Italy. [♦]Current address: University of Pennsylvania, Department of Chemistry, 231 South 34th Street, Philadelphia, PA 19104-6323. [×]Research project developed at the Istituto di Ricovero e Cura a Carattere Scientifico, Centro di Riferimento Oncologico della Basilicata, Via Padre Pio 1, I-85028 Rionero in Vulture, Potenza, Italy.

Received January 8, 2009

New arylthioindoles along with the corresponding ketone and methylene compounds were potent tubulin assembly inhibitors. As growth inhibitors of MCF-7 cells, sulfur derivatives were superior or sometimes equivalent to the ketones, while methylene derivatives were substantially less effective. Esters **24**, **27–29**, **36**, **39**, and **41** showed ~50% of inhibition on human HeLa and HCT116/chr3 cells at 0.5 μ M, and these compounds inhibited the growth of HEK, M14, and U937 cells with IC₅₀'s in the 78–220 nM range. While murine macrophage J774.1 cell growth was significantly less affected (20% at higher concentrations), four other nontransformed cell lines remained sensitive to these esters. The effect of drug treatment on cell morphology was examined by time-lapse microscopy. In a protocol set up to evaluate toxicity on the *Saccharomyces cerevisiae* BY4741 wild type strain, compounds **24** and **54** strongly reduced cell growth, and **29**, **36**, and **39** also showed significant inhibition.

Introduction

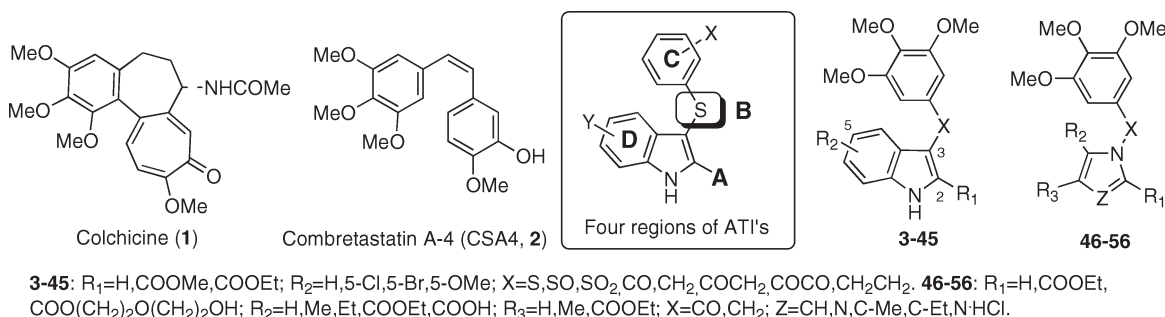
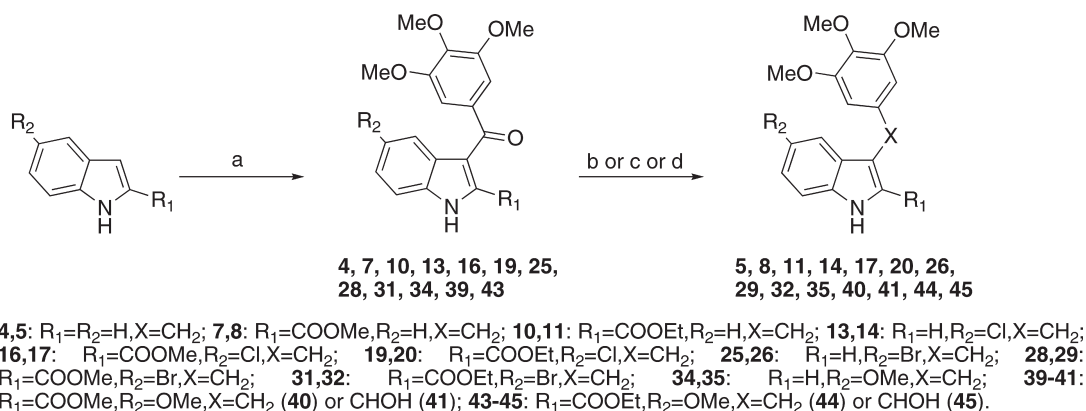
Microtubules are a key target for anticancer agents.¹ Tubulin interacting agents interfere with the dynamic equilibrium of microtubules by either inhibition of tubulin polymerization or blocking microtubule disassembly, and both effects lead cells to the arrest of cell division. Colchicine (**1**), combretastatin A-4 (CSA4,^a **2**), and the *Catharanthus* alkaloids vincristine and vinblastine are tubulin assembly inhibitors that interact with α,β -tubulin dimers at distinct interfaces between the two subunits^{2,3} (Chart 1). These interactions result in microtubule destabilization and subsequent

cellular apoptosis. Taxoids and epothilones target a luminal site on the β -subunit of dimers in microtubules^{4,5} and may enter the lumen through a binding site⁶ located at a pore on the microtubule surface formed by two different tubulin dimers. Paclitaxel stimulates microtubule polymerization and stabilization at high concentrations, whereas at lower concentrations the drug inhibits microtubule dynamics with little effect on the proportion of tubulin in polymer.^{7,8} Independent of precise mechanism of action, clinical use of antitubulin drugs is associated with problems of drug resistance, toxicity, and bioavailability.⁹

Arylthioindoles (ATIs) are potent tubulin assembly inhibitors that bind to the colchicine site on β -tubulin close to its interface with α -tubulin within the α,β -dimer.¹⁰ ATIs efficiently inhibit tubulin polymerization and cancer cell growth, with activities comparable with those of colchicine and CSA4. To rationalize the structure–activity relationship (SAR) studies, we dissected the ATI structure into four regions: (A) the substituent at position 2 of the indole, (B) the sulfur atom bridge, (C) the 3-arylthio group, and (D) the substituent at position 5 of the indole (Chart 1). In our previous papers, we reported SAR and molecular modeling studies on ATI derivatives differing in substituent groups and/or position at the A, C, and D regions.^{11,12} However, chemical modification of the sulfur bridge (B region) was not exhaustively explored,

*To whom correspondence should be addressed. Phone +39 06 4991 3800. Fax: +39 06 491 491. E-mail: romano.silvestri@uniroma1.it.

^aAbbreviations: ATI, arylthioindole; CSA4, combretastatin A-4; SAR, structure–activity relationship; MW, microwave; P_{max} , maximum pressure; TMSDM, trimethylsilyldiazomethane; MCPBA, 3-chloroperoxybenzoic acid; PPA, polyphosphoric acid; TBAHS, tetrabutylammonium hydrogen sulfate; DIPAD, diisopropyl azodicarboxylate; DMSO, dimethylsulfoxide; THF, tetrahydrofuran; MCF-7, human breast carcinoma cells; HeLa, cervical cancer cells from Henrietta Lacks; HCT116/chr3, human colon cancer cells; HEK, human embryonic kidney 293 cells; M14, human melanoma cells; U937, human monocytic leukemia cells; J774.1, murine macrophage cells; TLM, time-lapse microscopy, a slow process technique of photographing, which allows watching cellular growth; MTT, (3-(4,5-dimethylthiazol-2-yl)-2,5-diphenyltetrazolium bromide; PDB, protein data bank, DAMA-colchicine, *N*-deacetyl-*N*-(2-mercaptoacetyl)colchicine.

Chart 1. Structures of Derivatives **3–56** and Reference Compounds **1** and **2****Scheme 1.** Synthesis of Compounds **4, 5, 7, 8, 10, 11, 13, 14, 16, 17, 19, 20, 25, 26, 28, 29, 31, 32, 34, 35, 39–41** and **43–45**^a

^a Reagents and reaction conditions: (a) 3,4,5-trimethoxybenzoyl chloride, AlCl_3 , 1,2-dichloroethane, closed vessel, 110°C , 150 W, $P_{\text{max}} = 250$ PSI, 2 min, 40–68%; (b) (**5, 14, 26**, and **35**) NaBH_4 (10 equiv), EtOH, reflux, 3 h, 42–68%; (c) (**8, 11, 17, 20, 29, 32, 41**, and **45**) Et_3SiH , CF_3COOH , 25°C , overnight, 46–90%; (d) (**40** and **44**) NaBH_4 (1 equiv), THF/ H_2O , reflux, 2 h, 29–53%.

although five ATIs were transformed into the corresponding sulfur dioxides.¹¹ In contrast to the weak potency displayed by these dioxides,¹¹ several CSA4 analogues, characterized by a carbonyl functionality as a bridging group between the indole nucleus and the trimethoxyphenyl ring, show potent inhibition of tubulin polymerization.¹³ However, in comparing ATIs with the 3-aryloindoles reported by Hsieh and co-workers,¹⁴ we should note that these two groups of compounds are significantly different because there are major differences in our SAR findings and those of Hsieh's group. Moreover, our molecular modeling studies indicate that in the colchicine site of tubulin, ATI derivatives preferentially assume a colchicine-like rather than a CSA4-like binding conformation.^{10–12}

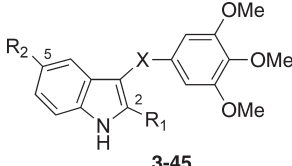
These observations prompted the SAR investigations at the B bridge reported here. To this end, we synthesized new indole derivatives by bioisosteric replacement of the sulfur bridge of the ATI's with either carbonyl or methylene moieties, and other related groups (compounds **3–45**, Table 1). In addition, we examined the replacement of the indole ring with differently substituted pyrrole and imidazole analogues (compounds **46–56**, Table 2).

Chemistry. Compounds **4, 7, 10, 13, 16, 19, 25, 28, 31, 34, 39**, and **43** were synthesized in a microwave (MW) reactor by treating the appropriate indole with 3,4,5-trimethoxybenzoyl chloride in the presence of aluminum chloride in 1,2-dichloroethane at 110°C (150 W) for 2 min (Scheme 1). Similarly, ethyl 5-chloro-3-[2-(3,4,5-trimethoxyphenyl)acetyl]-1H-indole-2-carboxylate **21** was prepared by MW synthesis using ethyl 5-chloro-1H-indole-2-carboxylate and 2-(3,4,5-trimethoxyphenyl)acetyl chloride. The latter reagent was obtained by treating the appropriate carboxylic

acid with oxalyl chloride in the presence of a catalytic amount of DMF in anhydrous THF at 0°C for 10 min (Scheme 2). Sodium borohydride (10 equiv) reduction of **4, 13, 25**, and **34** in boiling ethanol for 3 h furnished the corresponding benzyl derivatives **5, 14, 26**, and **35**, respectively (Scheme 1). Alternatively, benzyl (**8, 11, 17, 20, 29, 32, 41, 45**) and phenylethyl (**23**) derivatives were obtained in good yield by treating benzoyl (**7, 10, 16, 19, 28, 31, 39**, and **43**) (Scheme 1) or oxalyl (**22**) (Scheme 2) compounds with triethylsilane in trifluoroacetic acid at 25°C for 12 h. Reduction of ketones **39** and **43** with sodium borohydride (1 equiv) in refluxing aqueous THF for 2 h gave the corresponding alcohols **40** and **44**. MW oxidation of ethyl 3-[2-(3,4,5-trimethoxyphenyl)acetyl]-1H-indole-2-carboxylate (**21**) with selenium(IV) oxide in dimethylsulfoxide (DMSO) at 150°C (150 W) for 2 min furnished the corresponding 2-oxo derivative **22**.

Methyl (**27**) and ethyl (**30**) 5-bromo-3-(3,4,5-trimethoxyphenylthio)-1H-indole-2-carboxylate were obtained by MW reaction of 5-bromo-1H-indole-2-carboxylic acid (**59**) with bis-(3,4,5-trimethoxyphenyl)disulfide¹⁰ in the presence of sodium hydride in anhydrous DMF at 110°C (150 W) for 2 min (Scheme 3). The crude carboxylic acid was transformed into the corresponding methyl ester **27** with trimethylsilyldiazomethane (TMSDM) in dichloromethane/methanol at 25°C for 30 min or into the ethyl ester **30** with thionyl chloride in absolute ethanol at 65°C for 2 h.

Oxidation of methyl 5-methoxy-3-(3,4,5-trimethoxyphenylthio)-1H-indole-2-carboxylate (**36**)¹⁰ with 1 or 2 equiv of 3-chloroperoxybenzoic acid (MCPBA) in chloroform at

Table 1. Inhibition of Tubulin Polymerization, Growth of MCF-7 Human Breast Carcinoma Cells and Colchicine Binding by Compounds **3–45** and Reference Compound **2**


3–45

compd	R ₁	R ₂	X	tubulin ^a IC ₅₀ ± SD (μM)	MCF-7 ^b IC ₅₀ ± SD (nM)	inhibition colchicine binding ^c (% ± SD)
3	H	H	S	2.6 ± 0.2	34 ± 9	68 ± 0.8
4	H	H	C=O	3.5 ± 0.07	150 ± 50	26 ± 0.3
5	H	H	CH ₂	28 ± 2	nd	nd
6	COOMe	H	S	2.9 ± 0.1	25 ± 1	74 ± 2
7	COOMe	H	C=O	2.7 ± 0.3	33 ± 10	49 ± 10
8	COOMe	H	CH ₂	4.2 ± 0.02	190 ± 70	33 ± 7
9	COOEt	H	S	2.9 ± 0.2	40 ± 2	19 ± 7
10	COOEt	H	C=O	2.6 ± 0.3	80 ± 20	51 ± 6
11	COOEt	H	CH ₂	5.4 ± 1	nd	nd
12	H	5-Cl	S	2.6 ± 0.2	77 ± 7	51 ± 4
13	H	5-Cl	C=O	2.5 ± 0.5	53 ± 10	44 ± 9
14	H	5-Cl	CH ₂	24 ± 2	nd	nd
15	COOMe	5-Cl	S	2.5 ± 0.3	42 ± 10	73 ± 0.2
16	COOMe	5-Cl	C=O	1.6 ± 0.1	30 ± 6	61 ± 4
17	COOMe	5-Cl	CH ₂	1.7 ± 0.5	87 ± 30	49 ± 4
18	COOEt	5-Cl	S	2.2 ± 0.2	110 ± 2	53 ± 3
19	COOEt	5-Cl	C=O	1.4 ± 0.2	110 ± 10	49 ± 3
20	COOEt	5-Cl	CH ₂	2.5 ± 0.5	230 ± 60	39 ± 4
21	COOEt	5-Cl	COCH ₂	> 40	nd	nd
22	COOEt	5-Cl	COCO	> 40	nd	nd
23	COOEt	5-Cl	CH ₂ CH ₂	> 40	nd	nd
24	H	5-Br	S	1.6 ± 0.3	43 ± 7	65 ± 3
25	H	5-Br	C=O	1.9 ± 0.3	60 ^d	45 ± 5
26	H	5-Br	CH ₂	13 ± 0.8	nd	nd
27	COOMe	5-Br	S	0.99 ± 0.1	33 ± 10	75 ± 3
28	COOMe	5-Br	C=O	1.3 ± 0.08	18 ± 4	67 ± 4
29	COOMe	5-Br	CH ₂	1.3 ± 0.08	30 ± 9	59 ± 7
30	COOEt	5-Br	S	1.6 ± 0.2	83 ± 20	62 ± 7
31	COOEt	5-Br	C=O	1.6 ± 0.05	67 ± 10	58 ± 2
32	COOEt	5-Br	CH ₂	1.7 ± 0.2	100 ^d	53 ± 4
33	H	5-OMe	S	4.1 ± 0.6	22 ± 2	61 ± 4
34	H	5-OMe	C=O	3.4 ± 0.4	200 ^d	32 ± 7
35	H	5-OMe	CH ₂	14 ± 0.5	nd	nd
36	COOMe	5-OMe	S	2.0 ± 0.2	13 ± 3	93 ± 0.8
37	COOMe	5-OMe	S=O	> 40	nd	nd
38	COOMe	5-OMe	S(=O) ₂	> 40	nd	nd
39	COOMe	5-OMe	C=O	0.67 ± 0.02	17 ± 6	78 ± 6
40	COOMe	5-OMe	CHOH	> 40	nd	nd
41	COOMe	5-OMe	CH ₂	1.4 ± 0.2	33 ± 10	59 ± 1
42	COOEt	5-OMe	S	2.4 ± 0.2	46 ± 3	71 ± 2
43	COOEt	5-OMe	C=O	2.6 ± 0.04	90 ± 10	49 ± 4
44	COOEt	5-OMe	CHOH	> 40	nd	nd
45	COOEt	5-OMe	CH ₂	2.8 ± 0.3	93 ± 10	42 ± 4
2				1.1 ± 0.1	2.5 ± 0.6	99 ± 0.7

^a Inhibition of tubulin polymerization. Tubulin was 10 μM during polymerization. ^b Inhibition of growth of MCF-7 human breast carcinoma cells. ^c Inhibition of [³H]colchicine binding. Tubulin was at 1 μM, both [³H]colchicine and inhibitor were at 5 μM. ^d Same value obtained in all experiments.

25 °C for 1.5 h gave the corresponding sulfoxide (**37**) or sulfone (**38**) derivatives, respectively (Scheme 4). Ethyl 5-bromo-1*H*-indole-2-carboxylate (**59**) was prepared by intramolecular cyclization of the corresponding ethyl pyruvate 4-bromophenylhydrazone (**57**) in polyphosphoric acid (PPA) as a catalyst, according to Fischer's indole synthesis. The needed hydrazone **57** was obtained by MW reaction of 4-bromophenylhydrazine hydrochloride with ethyl pyruvate and sodium acetate in ethanol at 100 °C (250 W) for 5 min. MW hydrolysis of ester **58** with 3 N sodium hydroxide at 110 °C (150 W) for 1 min furnished 5-bromo-1*H*-indole-

2-carboxylic acid (**59**), which was transformed into the corresponding methyl ester **50** by treatment with thionyl chloride in anhydrous methanol at 65 °C for 2 h (Scheme 5).

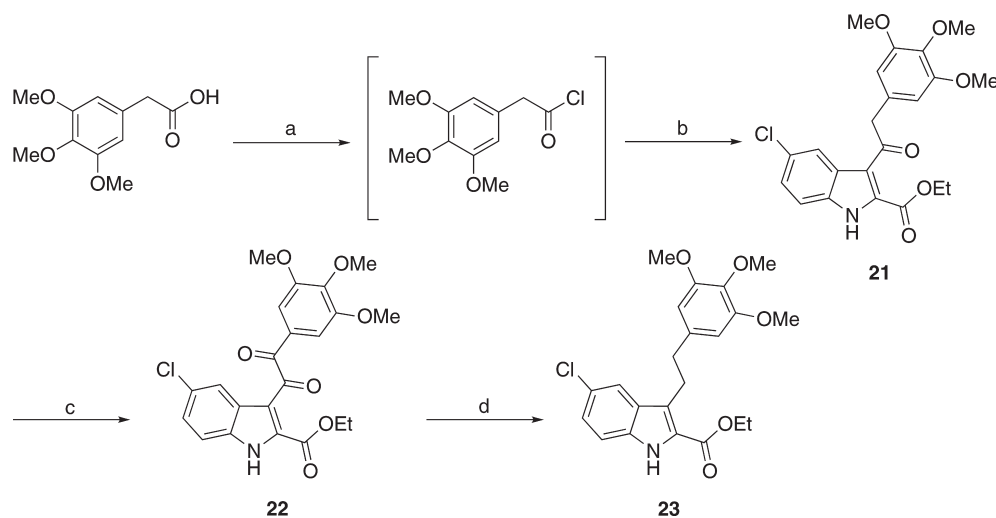
Compounds **46–49** were synthesized by phase-transfer reaction from an appropriate ethyl 1*H*-pyrrole-2-carboxylate and 3,4,5-trimethoxybenzyl chloride¹⁵ in the presence of tetrabutylammonium hydrogen sulfate (TBAHS) in 50% sodium hydroxide/dichloromethane. Reaction of 3,4,5-trimethoxybenzyl alcohol with ethyl 1*H*-imidazole-4-carboxylate in the presence of diisopropyl azodicarboxylate (DIPAD) according

Table 2. Inhibition of Tubulin Polymerization, Growth of MCF-7 Human Breast Carcinoma Cells by Compounds **46–56**, and Reference Compound **2**

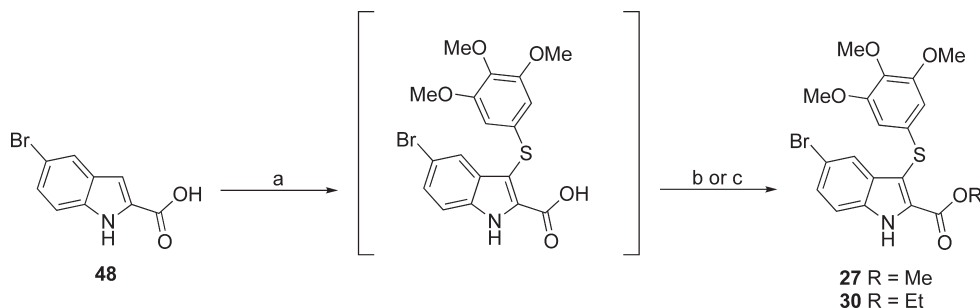
46-56

compd	R ₁	R ₂	R ₃	X	Y	tubulin ^a IC ₅₀ ± SD (μM)	MCF-7 ^b IC ₅₀ ± SD (nM)
46	COOEt	H	H	CH ₂	CH	> 40	nd
47	COOEt	H	Me	CH ₂	C-Me	> 40	nd
48	COOEt	Me	Me	CH ₂	C-Me	> 40	nd
49	COOEt	Et	Me	CH ₂	C-Et	> 40	nd
50	H	COOEt	H	CH ₂	N	> 40	nd
51	COOEt	H	H	C=O	CH	32 ± 0.6	> 2500
52	H	COOEt	H	C=O	N	> 40	> 2500
53	H	H	COOEt	C=O	N	> 40	> 2500
54	COOH	H	H	CH ₂	CH	> 40	> 2500
55	COO(CH ₂) ₂ O(CH ₂) ₂ OH	Me	Me	CH ₂	C-Me	> 40	nd
56	H	COOH	H	CH ₂	N·HCl	> 40	nd
2						1.1 ± 0.1	2.5 ± 0.6

^a Inhibition of tubulin polymerization. Tubulin was 10 μM during polymerization. ^b Inhibition of growth of MCF-7 human breast carcinoma cells.

Scheme 2. Synthesis of Compounds **21**, **22**, and **23**^a

^a Reagents and reaction conditions: (a) oxalyl chloride, anhydrous DMF cat., anhydrous THF, 0 °C, 10 min; (b) ethyl 5-chloro-1H-indole-2-carboxylate, AlCl₃, 1,2-dichloroethane, closed vessel, 110 °C, 150 W, P_{\max} = 250 PSI, 2 min, 32%; (c) selenium(IV) oxide, DMSO, closed vessel, 150 °C, 150 W, P_{\max} = 250 PSI, 2 min, 56%; (d) Et₃SiH, CF₃COOH, 25 °C, overnight, 40%.

Scheme 3. Synthesis of Compounds **27** and **30**^a

^a Reagents and reaction conditions: (a) NaH, bis(3,4,5-trimethoxyphenyl)disulfide, anhydrous DMF, closed vessel, 110 °C, 150 W, P_{\max} = 250 PSI, PowerMAX, 2 min; (b) (27) TMSDM, CH₂Cl₂/MeOH, 25 °C, 30 min, 79%; (c) (30) SOCl₂, absolute EtOH, 65 °C, 2 h, Ar stream, 70%.

to the Mitsunobu reaction¹⁶ afforded ethyl 1-(3,4,5-trimethoxybenzyl)-1H-imidazole-4-carboxylate (**50**). Reaction of 3,4,5-trimethoxybenzoyl chloride with ethyl 1H-pyrrole-2-

carboxylate in the presence of potassium *tert*-butoxide and 18-crown-6 or with ethyl 1H-imidazole-4-carboxylate gave ethyl 1-(3,4,5-trimethoxybenzoyl)-1H-pyrrole-2-carboxylate (**51**) or

little in activities from the corresponding sulfur/carbonyl compounds (compare **8** with **6** and **7**, **11** with **9** and **10**, **17** with **15** and **16**, **20** with **18** and **19**, **29** with **27** and **28**, **32** with **30** and **31**, **41** with **39** and **36**, and **45** with **43** and **42**). In contrast, when there was a hydrogen atom at position 2, there was a 3–11-fold reduction in inhibitory activity (compare **5** with **3** and **4**, **14** with **12** and **13**, **26** with **24** and **25**, and **35** with **33** and **34**). Seven compounds (**21**–**23**, **37**, **38**, **40**, and **44**) were completely inactive. These results clearly indicate forbidden chemical modifications at the B region, namely (i) elongation of the bridging group from 1 to 2 atomic units (compounds **21**–**23**), (ii) oxidation of the sulfur atom to oxide (**37**) or dioxide (**37** and **38**), as we also observed in our previous paper,¹¹ and (iii) reduction of the carbonyl bridge to an alcohol (**40** and **44**).

As growth inhibitors of MCF-7 human breast carcinoma cells, the sulfur derivatives were superior (compare **3** with **4**, **9** with **10**, **24** with **25**, **33** with **34**, and **42** with **43**) or equivalent (compare **6** with **7**, **12** with **13**, **15** with **16**, **18** with **19**, **27** with **28**, **30** with **31**, and **36** with **39**) to the corresponding ketones, while methylene derivatives were usually less effective (compare **8** with **6** and **7**, **17** with **15** and **16**, **20** with **18** and **19**, **29** with **27** and **28**, **32** with **30** and **31**, **41** with **39** and **36**, and **45** with **42** and **53**). (Generally, only inhibitors of tubulin polymerization with $IC_{50} < 5 \mu M$ were evaluated for inhibition of MCF-7 cell growth). The greatest inhibitory effects on MCF-7 cells were observed with either sulfur or carbonyl derivatives bearing a 2-methoxycarbonyl group at position 2 of the indole.

Compounds bearing either a bromine atom or a methoxy group at position 5 and a 2-methoxycarbonyl group at position 2 of the indole were found to be potent inhibitors in both the tubulin polymerization and MCF-7 cell growth assays, with potencies comparable to those of reference compound **2**. Worthy of note, among these esters, the methylene derivatives **29** and **41** were also highly active in both assays. In previous studies, ATIs showed comparable^{11,12} to greater¹⁰ inhibition of tubulin polymerization than **1** and adopted a binding orientation similar to that of DAMA-colchicine.¹⁰

Compounds that inhibited tubulin assembly with IC_{50} 's $< 5 \mu M$ were also evaluated for inhibition of the binding of [³H]colchicine to tubulin. Although none was as potent as CSA4, significant inhibition was observed with all active agents. As usually occurs with a series of antitubulin compounds, there was not a linear correlation between colchicine binding inhibition and inhibition of tubulin assembly. The most active inhibitor of colchicine binding was compound **36**, which was almost as active as CSA4, although the difference was more noticeable when the inhibitor concentration was $1 \mu M$ instead of $5 \mu M$ (data not presented). Compound **36** was about half as active as CSA4 as an inhibitor of assembly (IC_{50} 's of 2.0 and $1.1 \mu M$, respectively). Compounds **27** and **39**, both more active than CSA4 as inhibitors of assembly (IC_{50} 's of 0.99 and $0.67 \mu M$, respectively), were less active than **36** as inhibitors of colchicine binding.

We designed derivatives **46**–**56** for correlation with the structure of the ATIs by replacing the indole ring with differently substituted pyrrole and imidazole analogues (Table 2). Predictive docking studies suggested the synthesis of **46**–**56** because we observed a close overlap between their trimethoxyphenyl group and the corresponding ring A of the co-crystallized DAMA-colchicine in the colchicine site on tubulin. However, only **51** showed any inhibition of tubulin polymerization and, in keeping with its weak activity, **51** did not inhibit MCF-7 cell growth. An explanation of these

Table 3. Effects of **24**, **27**–**29**, **36**, **39**, and **41** on HeLa and HCT116/chr3 Cell Proliferation

compd	% of cell proliferation ^{a,b}			
	HeLa ^c		HCT116/chr3 ^d	
	0.5 μM	1 μM	0.5 μM	1 μM
24	47 ± 0.5	56 ± 1.2	60 ± 0.8	60 ± 3.9
27	53 ± 0.1	60 ± 0.1	57 ± 0.9	62 ± 1.9
28	41 ± 1.1	47 ± 0.4	59 ± 0.2	66 ± 3.5
29	52 ± 0.4	45 ± 1.6	51 ± 4.6	51 ± 1.6
36	57 ± 1.4	43 ± 0.3	63 ± 1.0	54 ± 1.0
39	55 ± 0.7	54 ± 0.3	57 ± 3.4	55 ± 1.2
41	52 ± 0.7	51 ± 0.2	69 ± 6.7	69 ± 0.3

^aData are expressed as % mean values ± SD; control cells are considered as 100% (MTT method). ^bTreatments were performed for 24 h at the indicated concentrations. ^cHeLa cervical cancer cells. ^dHCT116/chr3 human colon cancer cells.

Table 4. Inhibition of Growth of HEK, M14 and U937 Cells by Compounds **24**, **27**–**29**, **36**, **39**, and **41**^a

compd	$IC_{50} \pm SD$ (nM)		
	HEK ^b	M14 ^c	U937 ^d
24	220 ± 3	194 ± 3	100 ± 3
27	189 ± 5	155 ± 9	177 ± 10
28	131 ± 3	78 ± 3	191 ± 7
29	160 ± 5	120 ± 10	159 ± 10
36	128 ± 7	111 ± 6	122 ± 6
39	140 ± 1	100 ± 5	155 ± 10
41	181 ± 3	137 ± 5	189 ± 5

^aGrowth inhibition of the indicated cell lines (MTT method); incubation time was 48 h. ^bHEK, human embryonic kidney 293 cells; ^cM14, human melanoma cells; ^dU937, human leukemic monocyte lymphoma cells.

findings is suggested in the modeling section (see below). Surprisingly, compound **54**, which was inactive against bovine tubulin and MCF-7 cells, effectively inhibited growth of the *Saccharomyces cerevisiae* BY4741 strain. Perhaps **54** might interact with yeast tubulin, and this hypothesis is under investigation in our laboratories.

The potent esters **24**, **27**–**29**, **36**, **39**, and **41** were evaluated at 0.5 and $1.0 \mu M$ for cell growth inhibition on human HeLa and HCT116/chr3 cells, derived from a cervix uterine carcinoma and a colon carcinoma, respectively. All compounds caused about 50% growth inhibition at the lower concentration tested (Table 3).

Compounds **24**, **27**–**29**, **36**, **39**, and **41** also reduced the viability of HEK, M14, and U937 cells in a dose- and time-dependent manner with IC_{50} values ranging from 78 nM (**28**, M14 cells) to 220 nM (**24**, HEK cells) (Table 4). In contrast, at 300 nM, these compounds caused only 20% reduction in murine macrophage J744.1 cell growth compared with untreated controls (Figure 1S, Supporting Information). Thus these compounds were active in six cancer cell lines, but they showed a reduced cytotoxic effect on the nonmalignant murine macrophage J744.1 cells.

This observation with the J744.1 cells raised the possibility that there might be a differential effect of esters **24**, **27**–**29**, **36**, **39**, and **41** in malignant and nontransformed cells, which in turn would suggest the possibility of a potential improvement in the therapeutic index for the ATIs versus other antitubulin agents. Accordingly, we expanded our study of nontransformed cells to an epithelial line (PtK2, *Potorus tridactylis* kidney epithelial cells), two aortic smooth muscle lines (human and rat), and an endothelial line (human umbilical

Table 5. Inhibition of Growth and MCF-7 Selectivity Index of HAOSMC, PtK2, A10, and HUVEC Cells by Compounds **24**, **27–29**, **36**, **39**, and **41** and Reference Compounds **2** and Paclitaxel^a

compd	IC ₅₀ ± SD (nM)				
	MCF-7	HAOSMC ^b (MCF-7 SI) ^f	PtK2 ^c (MCF-7 SI)	A10 ^d (MCF-7 SI)	HUVEC ^e (MCF-7 SI)
24	43 ± 7	300 ± 200 (7.0)	230 ± 100 (5.3)	210 ± 100 (4.9)	400 ± 100 (9.3)
27	33 ± 10	100 ± 30 (3.0)	280 ± 30 (8.5)	230 ± 100 (7.0)	140 ± 20 (4.2)
28	18 ± 4	55 ± 40 (3.1)	110 ± 60 (6.1)	280 ± 40 (16)	150 ± 0 ^g (8.3)
29	30 ± 9	35 ± 7 (1.2)	270 ± 100 (9.0)	230 ± 100 (7.7)	140 ± 20 (4.7)
36	13 ± 3	15 ± 7.4 (1.2)	78 ± 50 (6.0)	70 ± 70 (5.4)	38 ± 30 (2.9)
39	17 ± 6	35 ± 7 (2.1)	190 ± 20 (11)	95 ± 80 (5.6)	110 ± 60 (6.5)
41	33 ± 10	70 ± 10 (2.1)	190 ± 200 (5.8)	130 ± 100 (3.9)	170 ± 50 (5.2)
2	2.5 ± 0.6	18 ± 4 (7.2)	1.0 ± 1 (0.4)	23 ± 10 (9.2)	5.0 ± 5 (2.0)
Ptx ^h	3.0 ± 0.5	6.0 ± 6 (2.0)	21 ± 8 (7.0)	38 ± 10 (13)	7.0 ± 4 (2.3)

^a Growth inhibition of the indicated cell lines. ^b HAOSMC: human aortic smooth muscle cells (ATCC CLR-1999). ^c PtK2: potorous tridactylis kidney epithelial cells (ATCC CLL-56). ^d A10, rat embryonic aortic smooth muscle cells (ATCC CRL-1476). ^e HUVEC: human umbilical vein endothelial cells (ATCC CRL-2873). ^f MCF-7 SI: selectivity index (SI) for each agent in each cell line versus the MCF-7 cells (IC₅₀ in specific cell line divided by IC₅₀ in MCF-7 cells; the higher the SI, the more resistant the nontransformed cell line relative to the MCF-7 cells). ^g Same value obtained in both experiments. ^h Ptx: paclitaxel.

vein endothelial cells). We also determined the effects of CSA4 and paclitaxel on the growth of these four lines (Table 5).

In all cases, except for compound **24** with the umbilical vein endothelial cells, the ATI's were more inhibitory than they had been with the J744.1 cells (that is, all IC₅₀'s were less than 300 nM). The cytotoxicity pattern with each agent was different, although compound **36** was the most cytotoxic and compound **24** was overall the least cytotoxic with these four nontransformed cell lines. We devised the MCF-7 SI as a test for the idea that the ATI's would have selective toxicity for a tumor cell line as compared with nonmalignant cells and as compared with previously described antitubulin agents. This hope, raised with the J744.1 macrophage cells, was not confirmed with the additional cell lines. The average SI was 4.8 with CSA4 and 6.1 with paclitaxel, although even with these two agents specific SI's differed from each other (the kidney epithelial cells were highly sensitive to CSA4, while both muscle lines were relatively resistant; with paclitaxel, the human muscle cells were most sensitive, the rat muscle cells most resistant). The average SI with the esters ranged from 4.3 with compound **41** to 7.3 with compound **28**. We conclude that there is no significant difference between compounds **24**, **27–29**, **36**, **39**, and **41** as compared with CSA4 and paclitaxel.

The effect of drug treatment on cell morphology was examined by time-lapse microscopy (TLM) using a Leica CTR6500 microscope. Cells were kept at 37 °C under a 5% carbon dioxide atmosphere for 48 h. The cytotoxic effects of compounds **24**, **27–29**, **36**, **39**, and **41** on HEK and M14 cell growth increased in a concentration- and time-dependent manner. Figure 1 shows the effects of **24**, **39**, and **41** after a 48 h treatment. Control HEK and M14 cell cultures displayed elongated bipolar or polygonal morphology, while a significant effect on cell morphology and 12–30% growth inhibition was already observed as early as 12 h after compound addition (data not shown). The treatment for 48 h with **24**, **39**, or **41** induced significant morphologic changes in both cell lines, which became rounded and developed large vacuoles. Moreover, cells of both lines were less elongated than the untreated

controls, and some cells that became rounded also had a tendency to detach from the substrate. Similar changes were observed after treatment with **27–29** and **36** (data not shown).

Saccharomyces cerevisiae budding yeast has been used to enhance understanding of fundamental cellular and molecular processes occurring in mammalian cells, including DNA replication, DNA recombination, cell division, protein turnover, vesicular trafficking, and mechanisms involved in longevity of cell life and cell death. Approximately 31% of yeast genes have a mammalian homologue, and an additional 30% of yeast genes show domain similarity.¹⁷ Potentially, yeast can be a powerful model for the development of cell death-directed drugs. For example, paclitaxel, arsenic, bleomycin, and valproate induce apoptotic phenotypes in yeast.¹⁸ Yeast has increased our understanding of the pathogenic role of human proteins in neurodegenerative diseases.¹⁹ Finally, Cassidy-Stone and co-workers²⁰ identified MDIVI-1 (mitochondrial division inhibitor-1) by yeast screens of chemical libraries.

Here we set up a protocol to evaluate the toxicity of compounds **24**, **27**, **28**, and **54** on BY4741, a standard laboratory wild type strain of *S. cerevisiae*. As shown in Figure 2, **24** and **54** strongly reduced the viability of the BY4741 strain cells, which were cell growth limited at the first dilution (the second showed limited cell growth). Compound **29** also showed significant BY4741 inhibition (cell growth was limited to the third dilution).

Despite the small test set used in this experiment, the ester functionality of **27–29** clearly caused a drop in activity as compared with the most potent compound **24** lacking the ester group. Even more striking is the contrast between the high activity of **54** with the yeast cells and its inactivity in the mammalian assays. Despite its inactivity with mammalian tubulin, it is unclear from docking studies why **54** does not bind in the colchicine site (see below). The biological behavior of **54** in yeast may indicate an interaction with fungal tubulin, or the activity of the compound in yeast may indicate an alternate target (manuscript in preparation).

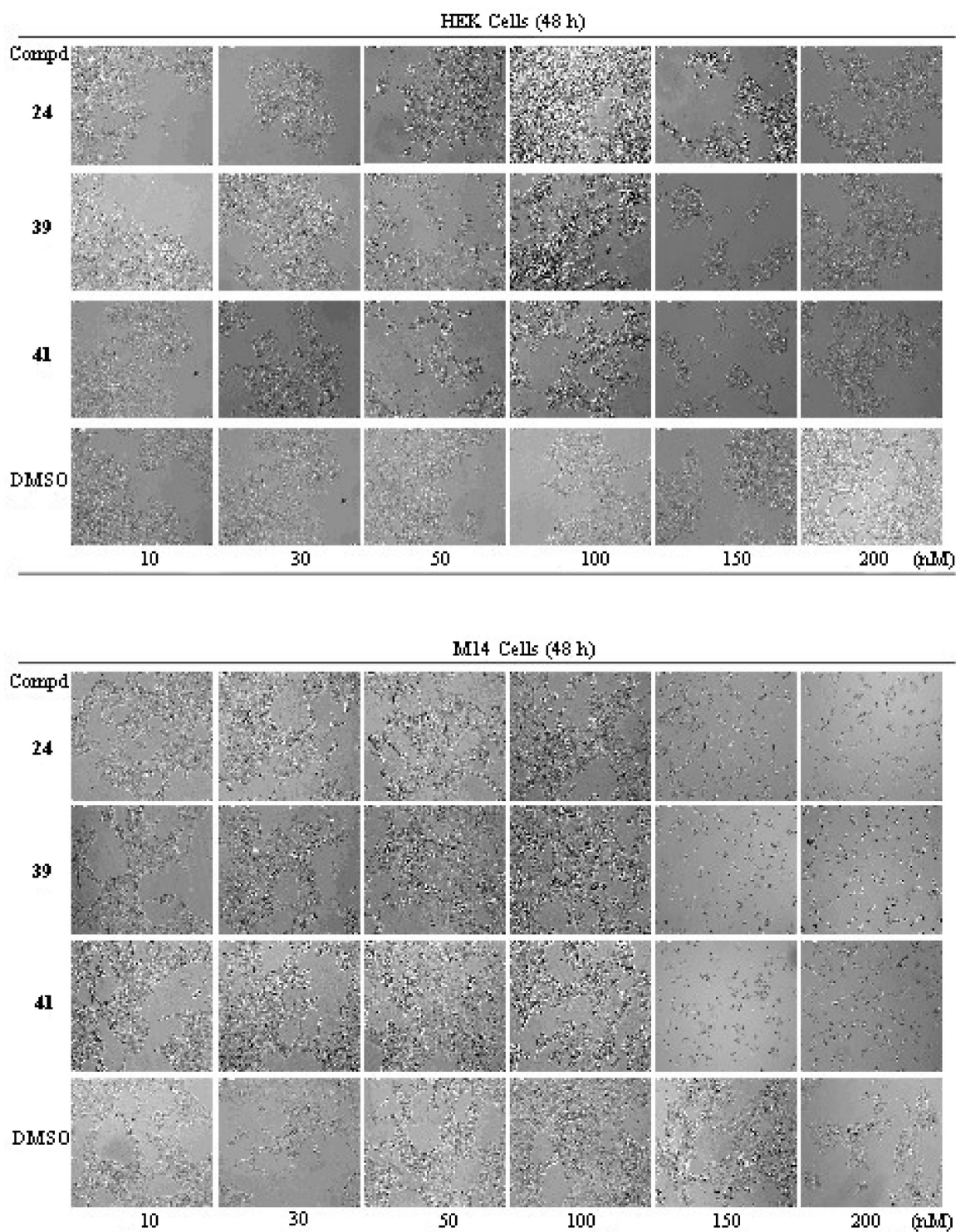


Figure 1. Effects of compounds **24**, **39**, and **41** on HEK (top) and M14 (bottom) cell morphology and growth as seen by TLM (magnification 10 \times).

Binding of Compounds to β -Tubulin in the Colchicine Site.

On the basis of our previous modeling results,^{10–12} we performed a series of docking simulations on a virtual library of structures with different bridges (B) in order to identify the most promising compounds before their actual synthesis. We also investigated *in silico* the potential of replacing the indole ring with smaller heterocycles such as pyrrole or imidazole.

The results obtained for the indole series showed that replacement of the sulfur atom in the bridge (B) with a

methylene or carbonyl moiety led to virtually identical docking poses as reported previously for ATIs. In particular, the trimethoxyphenyl moiety was situated in close proximity to Cys241, and the indole NH formed a hydrogen bond with Thr179 (Figure 3). These results predicted that these bridge modifications would lead to strong biological activity, and this was confirmed by the experimental results. Conversely, results for compounds with a two-carbon bridge were different. Such structures could not be correctly placed in the

colchicine site. The trimethoxyphenyl ring was more distant from Cys241, predicting poor binding and low biological activity. Consequently, we synthesized only three 2-carbon bridge analogues (**21–23**) to test the model, and the experimental data confirmed the predictions of the docking results (Table 1 data).

Replacement of the indole ring with differently substituted pyrrole and imidazole analogues led to less clear results. Most of the docked structures showed the trimethoxyphenyl group in a position similar to that of the corresponding ring A of the cocrystallized DAMA-colchicine. However, the heterocycle moieties were placed in different positions compared with the indole ring of the ATIs, and none of the poses

obtained showed any interaction with Thr179 (Figure 4). From these results, it was not easy to predict the potential activity of such compounds, and therefore a small series of pyrrole and imidazole analogues was prepared and tested experimentally. The biological data clearly showed that, in our model, the correct position of the trimethoxyphenyl group is necessary, but not sufficient, to predict the activity of novel compounds and that other structural features are required to have an accurate model. It should also be noted that our findings are in accord with the pharmacophore model previously developed for colchicine site compounds.²¹

Conclusions

Replacement of the sulfur atom of arylthioindoles with a carbonyl functionality led to compounds endowed with comparable inhibition of tubulin assembly. Replacement of the carbonyl with a methylene moiety led to inhibitors of tubulin assembly whose potency was dependent on the substituent at position 2 of the indole ring. As growth inhibitors of MCF-7 human breast carcinoma cells, sulfur derivatives were superior or equivalent to the ketones, while methylene derivatives were generally less effective. Compounds bearing either a bromine atom or a methoxy group at position 5 and the 2-methoxycarbonyl group at position 2 of the indole ring were potent inhibitors of both tubulin polymerization and MCF-7 cell growth, with potencies comparable to those of reference compound **2**. Two methylene derivatives, **29** and **41**, were also highly active in both assays. Esters **24**, **27–29**, **36**, **39**, and **41** showed ~50% inhibition of human HeLa and HCT116/chr3 cell growth at 0.5 μ M, and these compounds also reduced cell viability of HEK, M14, and U937 cells, with IC₅₀'s in the 78–220 nM range. In contrast, murine macrophage J744.1 cell growth was significantly less affected (20% at the highest concentrations). Four additional nontransformed cell lines, however, did not greatly differ in their sensitivity to compounds **24**, **27–29**, **36**, **39**, and **41**. The effect of drug treatment on cell morphology was examined by time-lapse microscopy. After 48 h, HEK and M14 cells treated with **24**, **27–29**, **36**, **39**,

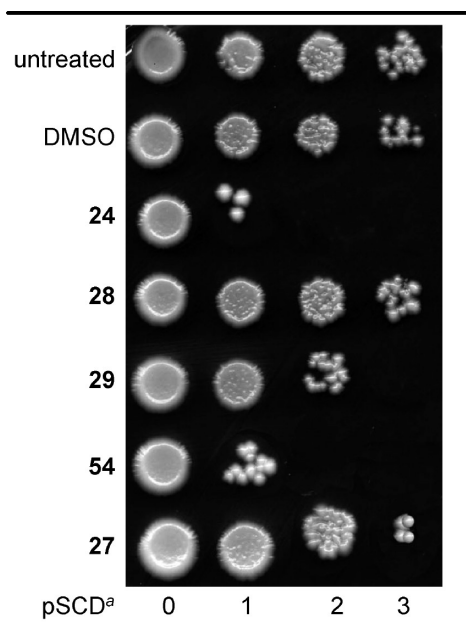


Figure 2. Effect of compounds **24**, **27–29**, and **54** on BY4741 wild type strain. Growth was recorded after 3 days at 28 °C; final compound concentration was 20 μ M. *a* = serial cell dilution (SCD).

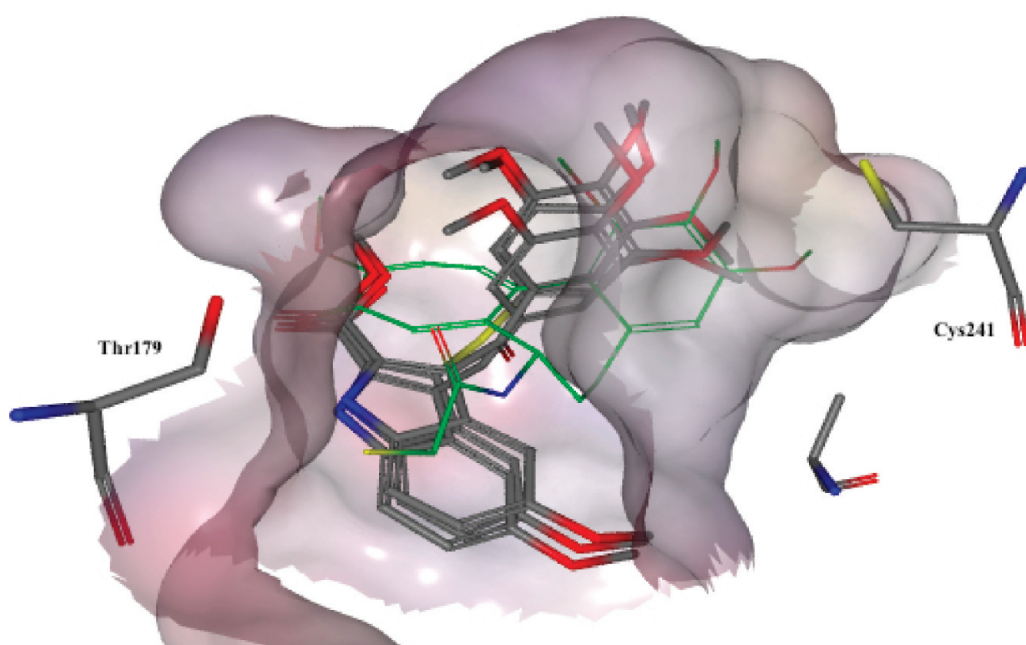


Figure 3. Docking poses for compounds **36**, **39**, and **41** (DAMA-colchicine in green).

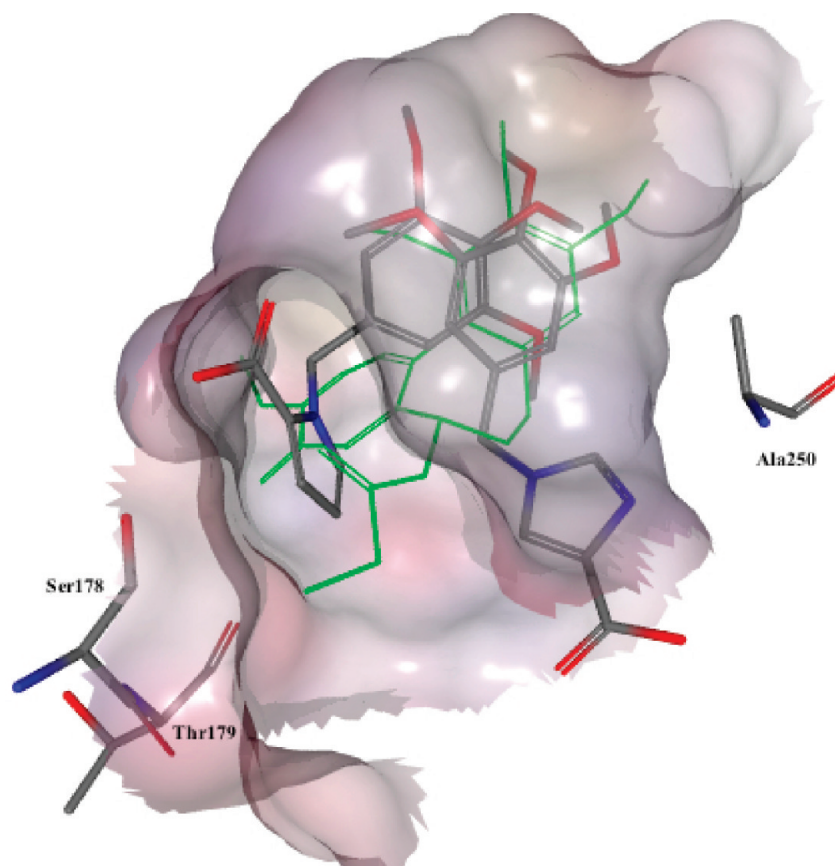


Figure 4. Docking poses for compounds **54** and **56** (compound **36** in green).

or **41** showed significant morphologic changes (cells became rounded with large vacuoles and with a tendency to detach from the substrate). In a protocol set up to evaluate compound toxicity on *S. cerevisiae* BY4741 wild type strain, compounds **24** and **54** strongly reduced cell growth, and **29**, **36**, and **39** also showed significant inhibitory effects. The strong activity of **54**, which was inactive against bovine tubulin and MCF-7 cells against BY4741 cells, requires further investigation.

Experimental Section

Chemistry. MW-assisted reactions were performed on Discover LabMate (CEM), setting temperature, irradiation power, maximum pressure (P_{max}), PowerMAX (in situ cooling during the MW irradiation), ramp and hold times, and open and closed vessel modes as indicated. Melting points (mp) were determined on a Buchi 510 apparatus and are uncorrected. Infrared spectra (IR) were run on a SpectrumOne FT-ATR spectrophotometer. Band position and absorption ranges are given in cm⁻¹. Proton nuclear magnetic resonance (¹H NMR) spectra were recorded on Bruker 200 and 400 MHz FT spectrometers in the indicated solvent. Chemical shifts are expressed in δ units (ppm) from tetramethylsilane. Column chromatography was performed on columns packed with alumina from Merck (70–230 mesh) or silica gel from Macherey-Nagel (70–230 mesh). Aluminum oxide TLC cards from Fluka (aluminum oxide precoated aluminum cards with fluorescent indicator visualizable at 254 nm) and silica gel TLC cards from Macherey-Nagel (silica gel precoated aluminum cards with fluorescent indicator visualizable at 254 nm) were used for thin layer chromatography (TLC). Developed plates were visualized by a Spectroline ENF 260C/F UV apparatus. Organic solutions were dried over anhydrous sodium sulfate. Evaporation of the solvents was carried out on a

Buchi Rotavapor R-210 equipped with a Buchi V-850 vacuum controller and Buchi V-700 and V-710 vacuum pumps. Elemental analyses of the biologically tested compounds were found within $\pm 0.4\%$ of the theoretical values. Purity of tested compounds was $> 95\%$. Compounds **3**,¹² **6**,¹⁰ **9**,¹⁰ **12**,¹² **15**,¹⁰ **18**,¹¹ **24**,¹² **33**,¹² **36**,¹⁰ and **42**¹¹ were prepared as previously reported.

General Procedure for the Synthesis of Compounds 4, 7, 10, 13, 16, 19, 21, 25, 28, 31, 34, 39, and 43. Example: (1*H*-Indol-3-yl)-(3,4,5-trimethoxyphenyl)methanone (**4**). A mixture of AlCl₃ (0.57 g; 0.0043 mol), the appropriate 1*H*-indole (0.5 g, 0.0043 mol) and 3,4,5-trimethoxybenzoyl chloride (0.99 g, 0.0043 mol) in 1,2-dichloroethane (2 mL) was placed into the MW cavity (closed vessel mode, P_{max} = 250 PSI). MW irradiation of 150 W was used, the temperature being ramped from 25 to 110 °C while stirring. Once 110 °C was reached, taking about 1 min, the reaction mixture was held at this temperature for 2 min, then cooled, diluted cautiously with water, and extracted with chloroform; the organic layer was washed with brine, dried, and filtered. Removal of the solvent gave a residue that was purified by silica gel column chromatography (ethyl acetate:*n*-hexane = 1:1 as eluent) to furnish **4** as a white solid (0.71 g, 53%), mp 210–213 °C (from ethanol), differing from lit.²² 174–176 °C and lit.²³ 132–133 °C. ¹H NMR (DMSO-*d*₆): δ 3.73 (s, 3H), 3.83 (s, 6H), 7.06 (s, 2H), 7.20–7.24 (m, 2H), 7.48 (d, *J* = 9.1 Hz, 1H), 8.06 (d, *J* = 3.0 Hz, 1H), 8.21 (d, *J* = 8.5 Hz, 1H), 11.99 ppm (broad s, disappeared on treatment with D₂O, 1H). IR: ν 1571, 3179 cm⁻¹.

Methyl 3-(3,4,5-trimethoxybenzoyl)-1*H*-indole-2-carboxylate (7). Synthesized as **4**, starting from methyl 1*H*-indole-2-carboxylate, yield 55%, yellow solid, mp 163–168 °C (from ethanol/water). ¹H NMR (DMSO-*d*₆): δ 3.52 (s, 3H), 3.73 (s, 6H), 3.74 (s, 3H), 7.03 (s, 2H), 7.17 (t, *J* = 7.2 Hz, 1H), 7.34 (t, *J* = 7.2 Hz, 1H), 7.54 (d, *J* = 7.5 Hz, 1H), 7.60 (d, *J* = 7.3 Hz, 1H), 12.56 ppm (broad s, disappeared on treatment with D₂O, 1H). IR: ν 1634, 1710, 3279 cm⁻¹. Anal. (C₂₀H₁₉NO₆ (369.37)) C, H, N.

Ethyl 3-(3,4,5-Trimethoxybenzoyl)-1H-indole-2-carboxylate (10). Synthesized as **4**, starting from ethyl 5-methoxy-1H-indole-2-carboxylate, yield 39%, white solid, mp 105–110 °C (ethanol/*n*-hexane). ¹H NMR (CDCl₃): δ 1.01 (t, *J* = 7.1 Hz, 3H), 3.82 (s, 6H), 3.93 (s, 3H), 4.14 (q, *J* = 7.1 Hz, 2H), 7.18 (s, 2H), 7.24 (t, *J* = 7.1 Hz, 1H), 7.41 (t, *J* = 7.1 Hz, 1H), 7.5 (d, *J* = 8.3 Hz, 1H), 7.73 (d, *J* = 8.1 Hz, 1H), 9.26 ppm (broad s, disappeared on treatment with D₂O, 1H). IR: ν 1648, 1686, 3303 cm⁻¹. Anal. (C₂₁H₂₁NO₆ (383.39)) C, H, N.

(5-Chloro-1H-indol-3-yl)-(3,4,5-trimethoxyphenyl)methanone (13). Synthesized as **4**, starting from 5-chloro-1H-indole, yield 68%, white solid, mp 240–245 °C (from ethanol). ¹H NMR (DMSO-*d*₆): δ 3.76 (s, 3H), 3.86 (s, 6H), 7.09 (s, 2H), 7.28 (dd, *J* = 8.7 Hz, 1H), 7.54 (t, *J* = 8.1 Hz, 1H), 8.19 (s, 1H), 8.23 (d, *J* = 2.2 Hz, 1H), 12.21 ppm (broad s, disappeared on treatment with D₂O, 1H). IR: ν 1600, 3261 cm⁻¹. Anal. (C₁₈H₁₆ClNO₄ (345.78)) C, H, Cl, N.

Methyl 5-Chloro-3-(3,4,5-trimethoxybenzoyl)-1H-indole-2-carboxylate (16). Synthesized as **4**, starting from methyl 5-chloro-1H-indole-2-carboxylate, yield 68%, yellow solid, mp 188–193 °C (from ethanol/water). ¹H NMR (CDCl₃): δ 3.69 (s, 3H), 3.84 (s, 6H), 3.96 (s, 3H), 7.16 (s, 2H), 7.36 (dd, *J* = 8.8 Hz, 1H), 7.44 (t, *J* = 8.8 Hz, 1H), 7.66 (d, *J* = 1.9 Hz, 1H), 9.50 ppm (broad s, disappeared on treatment with D₂O, 1H). IR: ν 1645, 1711, 3259 cm⁻¹. Anal. (C₂₀H₁₈ClNO₆ (403.81)) C, H, Cl, N.

Ethyl 5-Chloro-3-(3,4,5-trimethoxybenzoyl)-1H-indole-2-carboxylate (19). Synthesized as **4**, starting from ethyl 5-chloro-1H-indole-2-carboxylate, yield 38%, yellow solid, mp 160–163 °C (from ethanol). ¹H NMR (DMSO-*d*₆): δ 0.86 (t, *J* = 7.1 Hz, 3H), 3.73 (s, 3H), 3.75 (s, 6H), 3.96 (q, *J* = 7.1 Hz, 2H), 7.04 (s, 2H), 7.38 (dd, *J* = 10.1 Hz, 1H), 7.58 (d, *J* = 7.4 Hz, 1H), 7.69 (d, *J* = 2.1 Hz, 1H), 12.78 ppm (broad s, disappeared on treatment with D₂O, 1H). IR: ν 1636, 1684, 3294 cm⁻¹. Anal. (C₂₁H₂₀ClNO₆ (417.84)) C, H, Cl, N.

Ethyl 5-Chloro-3-(2-(3,4,5-trimethoxyphenyl)acetyl)-1H-indole-2-carboxylate (21). Synthesized as **4**, starting from ethyl 5-chloro-1H-indole-2-carboxylate and 2-(3,4,5-trimethoxyphenyl)acetyl chloride, yield 32%, yellow solid, mp 129–134 °C (from ethanol). ¹H NMR (CDCl₃): δ 1.46 (t, *J* = 7.1 Hz, 3H), 3.80 (s, 6H), 3.83 (s, 3H), 4.40 (s, 2H), 4.50 (q, *J* = 7.1 Hz, 2H), 6.46 (s, 2H), 7.32 (dd, *J* = 8.8 Hz, 1H), 7.33 (dd, *J* = 9.5 Hz, 1H), 7.96 (d, *J* = 1.8 Hz, 1H), 9.22 ppm (broad s, disappeared on treatment with D₂O, 1H). IR: ν 1641, 1721, 3169 cm⁻¹. Anal. (C₂₂H₂₂ClNO₆ (431.87)) C, H, Cl, N.

(5-Bromo-1H-indol-3-yl)-(3,4,5-trimethoxyphenyl)methanone (25). Synthesized as **4**, starting from 5-bromo-1H-indole, yield 53%, yellow solid, mp 235–240 °C (from ethanol). ¹H NMR (DMSO-*d*₆): δ 3.76 (s, 3H), 3.86 (s, 6H), 7.09 (s, 2H), 7.40 (dd, *J* = 6.6 Hz, 1H), 7.50 (d, *J* = 8.1 Hz, 1H), 8.18 (s, 1H), 8.39 (d, *J* = 2.5 Hz, 1H), 12.19 ppm (broad s, disappeared on treatment with D₂O, 1H). IR: ν 1599, 3279 cm⁻¹. Anal. (C₁₈H₁₆BrNO₄ (390.23)) C, H, Br, N.

Methyl 5-Bromo-3-(3,4,5-trimethoxybenzoyl)-1H-indole-2-carboxylate (28). Synthesized as **4**, starting from **49**, yield 40%, white solid, mp 207–210 °C (from ethanol/*n*-hexane). ¹H NMR (CDCl₃): δ 3.68 (s, 3H), 3.83 (s, 6H), 3.95 (s, 3H), 7.14 (s, 2H), 7.38 (d, *J* = 8.2 Hz, 1H), 7.48 (dd, *J* = 6.9 Hz, 1H), 7.81 (d, *J* = 1.8 Hz, 1H), 9.45 ppm (broad s, disappeared on treatment with D₂O, 1H). IR: ν 1642, 1711, 3248 cm⁻¹. Anal. (C₂₀H₁₈BrNO₆ (448.26)) C, H, Br, N.

Ethyl 5-Bromo-3-(3,4,5-trimethoxybenzoyl)-1H-indole-2-carboxylate (31). Synthesized as **4**, starting from **48**, yield 46%, yellow solid, mp 135–140 °C (from ethanol/*n*-hexane). ¹H NMR (DMSO-*d*₆): δ 0.85 (t, *J* = 7.1 Hz, 3H), 3.73 (s, 3H), 3.75 (s, 6H), 3.98 (q, *J* = 7.1 Hz, 2H), 7.03 (s, 2H), 7.33 (d, *J* = 1.2 Hz, 1H), 7.48 (dd, *J* = 6.9 Hz, 1H), 7.53 (dd, *J* = 8.8 Hz, 1H), 12.74 ppm (broad s, disappeared on treatment with D₂O, 1H). IR: ν 1638, 1702, 3292 cm⁻¹. Anal. (C₂₁H₂₀BrNO₆ (462.29)) C, H, Br, N.

(5-Methoxy-1H-indol-3-yl)-(3,4,5-trimethoxyphenyl)methanone (34). Synthesized as **4**, starting from 5-methoxy-1H-indole, yield 42%, yellow solid, mp 202–207 °C (from ethanol), lit.¹⁴ 194–195 °C.

Methyl 5-Methoxy-3-(3,4,5-trimethoxybenzoyl)-1H-indole-2-carboxylate (39). Synthesized as **4**, starting from methyl 5-methoxy-1H-indole-2-carboxylate, yield 20%, yellow solid, mp 168–173 °C (from ethanol/water). ¹H NMR (DMSO-*d*₆): δ 3.47 (s, 3H), 3.71 (s, 3H), 3.73 (s, 3H), 3.74 (s, 6H), 6.99–7.02 (m, 3H), 7.07 (d, *J* = 2.3 Hz, 1H), 7.44 (d, *J* = 8.95 Hz, 1H), 12.49 ppm (broad s, disappeared on treatment with D₂O, 1H). IR: ν 1635, 1710, 3274 cm⁻¹. Anal. (C₂₁H₂₁NO₇ (399.39)) C, H, N.

Ethyl 5-Methoxy-3-(3,4,5-trimethoxybenzoyl)-1H-indole-2-carboxylate (43). Synthesized as **4**, starting from ethyl 5-methoxy-1H-indole-2-carboxylate, yield 60%, yellow solid, mp 150–155 °C (from ethanol). ¹H NMR (CDCl₃): δ 0.97 (t, *J* = 7.1 Hz, 3H), 3.82 (s, 3H), 3.84 (s, 6H), 3.94 (s, 3H), 4.09 (q, *J* = 7.1 Hz, 2H), 7.07 (dd, *J* = 6.5 Hz, 1H), 7.18 (s, 2H), 7.26 (d, *J* = 1.9 Hz, 1H), 7.39 (d, *J* = 9.0 Hz, 1H), 9.21 ppm (broad s, disappeared on treatment with D₂O, 1H). IR: ν 1647, 1694, 3353 cm⁻¹. Anal. (C₂₂H₂₃NO₇ (413.42)) C, H, N.

General Procedure for the Synthesis of Compounds 5, 14, 26, and 35. Example: **3-(3,4,5-trimethoxybenzyl)-1H-indole (5).** Sodium borohydride (0.80 g, 0.021 mol) was added to a solution of **4** (0.66 g, 0.0021 mol) in ethanol (85 mL). The reaction mixture was refluxed for 3 h, then cooled, cautiously diluted with water, and extracted with ethyl acetate; the organic layer was washed with brine, dried, and filtered. Evaporation of the solvent gave a residue that was purified by silica gel column chromatography (ethyl acetate:*n*-hexane = 1:1 as eluent) to furnish **5** as a white solid (0.26 g, 42%), mp 133–136 °C (from ethanol), lit.²² 125–126 °C and lit.²⁴ 128–130 °C.

5-Chloro-3-(3,4,5-trimethoxybenzyl)-1H-indole (14). Synthesized as **5** starting from **13**, yield 47%, orange solid, mp 145–150 °C (from ethanol). ¹H NMR (CDCl₃): δ 3.80 (s, 6H), 3.83 (s, 3H), 4.00 (s, 2H), 6.49 (s, 2H), 6.95 (d, *J* = 2.3 Hz, 1H), 7.14 (dd, *J* = 8.6 Hz, 1H), 7.28 (d, *J* = 8.1 Hz, 1H), 7.51 (d, *J* = 2.0 Hz, 1H), 8.40 ppm (broad s, disappeared on treatment with D₂O, 1H). IR: ν 3372 cm⁻¹. Anal. (C₁₈H₁₈ClNO₃ (331.79)) C, H, Cl, N.

5-Bromo-3-(3,4,5-trimethoxybenzyl)-1H-indole (26). Synthesized as **5**, starting from **25**, yield 58%, white solid, mp 145–150 °C (from ethanol). ¹H NMR (CDCl₃): δ 3.81 (s, 6H), 3.84 (s, 3H), 4.01 (s, 2H), 6.50 (s, 2H), 6.94 (d, *J* = 2.3 Hz, 1H), 7.24–7.28 (m, 2H), 7.69 (d, *J* = 1.7 Hz, 1H), 8.05 ppm (broad s, disappeared on treatment with D₂O, 1H). IR: ν 3353 cm⁻¹. Anal. (C₁₈H₁₈BrNO₃) C, H, Br, N.

5-Methoxy-3-(3,4,5-trimethoxybenzyl)-1H-indole (35). Synthesized as **5**, starting from **34**, yield 68%, white solid, mp 110–113 °C (from ethanol). ¹H NMR (CDCl₃): δ 3.78 (s, 6H), 3.80 (s, 3H), 3.81 (s, 3H), 4.01 (s, 2H), 6.51 (s, 2H), 6.84 (d, *J* = 8.8 Hz, 1H), 6.88 (t, *J* = 2.4 Hz, 1H), 6.97 (d, *J* = 2.4 Hz, 1H), 7.24 (t, *J* = 4.7 Hz, 1H), 7.90 ppm (broad s, disappeared on treatment with D₂O, 1H). IR: ν 3365 cm⁻¹. Anal. (C₁₉H₂₁NO₄ (327.37)) C, H, N.

General Procedure for the Synthesis of Compounds 8, 11, 17, 20, 23, 29, 32, 41, and 45. Example: **Methyl 3-(3,4,5-trimethoxybenzyl)-1H-indole-2-carboxylate (8).** To a cold solution of **7** (0.31 g, 0.00084 mol) in trifluoroacetic acid (0.96 g, 0.65 mL, 0.0084 mol) was added dropwise triethylsilane (0.22 g, 0.30 mL, 0.0019 mol). The reaction mixture was stirred at 25 °C for 24 h, then neutralized with a saturated solution of sodium hydrogen carbonate and extracted with ethyl acetate; the organic layer was washed with brine, dried, and filtered. Removal of the solvent gave a residue that was purified by silica gel column chromatography (ethyl acetate:*n*-hexane = 3:2 as eluent) to furnish **8** as a yellow solid (0.15 g, 50%), mp 156–161 °C (from ethanol/*n*-hexane). ¹H NMR (CDCl₃): δ 3.69 (s, 6H), 3.72 (s, 3H), 3.89 (s, 3H), 4.38 (s, 2H), 6.46 (s, 2H), 7.05 (t, *J* = 8.1 Hz, 1H), 7.25 (t, *J* = 8.3 Hz, 1H), 7.33 (d, *J* = 7.4 Hz, 1H), 7.57

(d, $J = 8.2$ Hz, 1H), 8.75 ppm (broad s, disappeared on treatment with D_2O , 1H). IR: ν 1690, 3318 cm^{-1} . Anal. ($C_{20}H_{21}NO_5$ (355.38)) C, H, N.

Ethyl 3-(3,4,5-Trimethoxybenzyl)-1H-indole-2-carboxylate (11). Synthesized as **8**, starting from **10**, yield 73%, white solid, mp 115–118 °C (from ethanol/*n*-hexane). 1H NMR ($CDCl_3$): δ 1.42 (t, $J = 7.1$ Hz, 3H), 3.77 (s, 6H), 3.80 (s, 3H), 4.44 (q, $J = 7.1$ Hz, 2H), 4.47 (s, 2H), 6.55 (s, 2H), 7.13 (t, $J = 7.0$ Hz, 1H), 7.33 (t, $J = 6.9$ Hz, 1H), 7.39 (d, $J = 7.5$ Hz, 1H), 7.64 (d, $J = 7.4$ Hz, 1H), 8.82 ppm (broad s, disappeared on treatment with D_2O , 1H). IR: ν 1672, 3337 cm^{-1} . Anal. ($C_{21}H_{23}NO_5$ (369.41)) C, H, N.

Methyl 5-Chloro-3-(3,4,5-trimethoxybenzyl)-1H-indole-2-carboxylate (17). Synthesized as **8**, starting from **16**, yield 69%, white solid, mp 172–175 °C (from ethanol/*n*-hexane). 1H NMR ($CDCl_3$): δ 3.70 (s, 6H), 3.73 (s, 3H), 3.89 (s, 3H), 4.33 (s, 2H), 6.42 (s, 2H), 7.21 (d, $J = 1.9$ Hz, 1H), 7.24 (t, $J = 8.7$ Hz, 1H), 7.51 (d, $J = 1.9$ Hz, 1H), 8.74 ppm (broad s, disappeared on treatment with D_2O , 1H). IR: ν 1682, 3322 cm^{-1} . Anal. ($C_{20}H_{20}ClNO_5$ (389.83)) C, H, Cl, N.

Ethyl 5-Chloro-3-(3,4,5-trimethoxybenzyl)-1H-indole-2-carboxylate (20). Synthesized as **8**, starting from **19**, yield 95%, yellow solid, mp 147–150 °C (from ethanol/*n*-hexane). 1H NMR ($CDCl_3$): δ 1.41 (t, $J = 7.1$ Hz, 3H), 3.79 (s, 6H), 3.81 (s, 3H), 4.41 (s, 2H), 4.43 (q, $J = 6.4$ Hz, 2H), 6.51 (s, 2H), 7.25–7.28 (m, 1H), 7.33 (dd, $J = 8.1$ Hz, 1H), 7.59–7.60 (m, 1H), 8.91 ppm (broad s, disappeared on treatment with D_2O , 1H). IR: ν 1666, 3315 cm^{-1} . Anal. ($C_{21}H_{22}ClNO_5$) C, H, Cl, N.

Ethyl 5-Chloro-3-(3,4,5-trimethoxyphenethyl)-1H-indole-2-carboxylate (23). Synthesized as **8**, starting from **22**, yield 40%, white solid, mp 163–165 °C (from ethanol). 1H NMR ($CDCl_3$): δ 1.44 (t, $J = 7.5$ Hz, 3H), 2.88 (t, $J = 7.4$ Hz, 2H), 3.35 (t, $J = 7.3$ Hz, 2H), 3.79 (s, 6H), 3.83 (s, 3H), 4.42 (t, $J = 7.1$ Hz, 2H), 6.38 (s, 2H), 7.24 (dd, $J = 9.2$ Hz, 1H), 7.31 (d, $J = 8.8$ Hz, 1H), 7.49 (d, $J = 1.9$ Hz, 1H), 9.01 ppm (broad s, disappeared on treatment with D_2O , 1H). IR: ν 1669, 3318 cm^{-1} . Anal. ($C_{22}H_{24}ClNO_5$ (417.88)) C, H, Cl, N.

Methyl 5-Bromo-3-(3,4,5-trimethoxybenzyl)-1H-indole-2-carboxylate (29). Synthesized as **8**, starting from **28**, yield 97%, yellow solid, mp 177–182 °C (from ethanol/*n*-hexane). 1H NMR ($DMSO-d_6$): δ 3.57 (s, 3H), 3.67 (s, 6H), 3.92 (s, 3H), 4.34 (s, 2H), 6.62 (s, 2H), 7.36–7.36 (m, 2H), 7.90 (d, $J = 2.3$ Hz, 1H), 11.88 ppm (broad s, disappeared on treatment with D_2O , 1H). IR: ν 1675, 3322 cm^{-1} . Anal. ($C_{20}H_{20}BrNO_5$ (434.28)) C, H, Br, N.

Ethyl 5-Bromo-3-(3,4,5-trimethoxybenzyl)-1H-indole-2-carboxylate (32). Synthesized as **8**, starting from **31**, yield 46%, white solid, mp 150–155 °C (from ethanol/*n*-hexane). 1H NMR ($CDCl_3$): δ 1.41 (t, $J = 7.1$ Hz, 3H), 3.79 (s, 6H), 3.82 (s, 3H), 4.43 (q, $J = 7.1$ Hz, 2H), 6.51 (s, 2H), 7.28 (d, $J = 9.4$ Hz, 1H), 7.29 (s, 2H), 7.40 (dd, $J = 6.9$ Hz, 1H), 7.77 (d, $J = 1.8$ Hz, 1H), 8.90 ppm (broad s, disappeared on treatment with D_2O , 1H). IR: ν 1665, 3317 cm^{-1} . Anal. ($C_{21}H_{22}BrNO_6$ (448.31)) C, H, Br, N.

Methyl 5-Methoxy-3-(3,4,5-trimethoxybenzyl)-1H-indole-2-carboxylate (41). Synthesized as **8**, starting from **39**, yield 58%, white solid, mp 125–128 °C (from ethanol/*n*-hexane). 1H NMR ($CDCl_3$): δ 3.77 (s, 6H), 3.79 (s, 3H), 3.80 (s, 3H), 3.94 (s, 3H), 4.42 (s, 2H), 6.53 (s, 1H), 6.96 (d, $J = 2.3$ Hz, 1H), 7.00 (dd, $J = 6.4$ Hz, 1H), 7.28 (d, $J = 8.9$ Hz, 1H), 8.67 (s, 1H), 11.91 ppm (broad s, disappeared on treatment with D_2O , 1H). IR: ν 1687, 3331 cm^{-1} . Anal. ($C_{21}H_{23}NO_6$ (385.41)) C, H, N.

Ethyl 5-Methoxy-3-(3,4,5-trimethoxybenzyl)-1H-indole-2-carboxylate (45). Synthesized as **8**, starting from **43**, yield 90%, white solid, mp 132–135 °C (from ethanol). 1H NMR ($CDCl_3$): δ 1.42 (t, $J = 7.1$ Hz, 3H), 3.78 (s, 9H), 3.81 (s, 3H), 4.44 (q, $J = 7.2$ Hz, 2H), 4.45 (s, 2H), 6.56 (s, 2H), 6.98–7.03 (m, 2H), 7.28–7.32 (m, 1H), 8.76 ppm (broad s, disappeared on treatment with D_2O , 1H). IR: ν 1672, 3330 cm^{-1} . Anal. ($C_{22}H_{25}NO_6$ (399.44)) C, H, N.

General Procedure for the Synthesis of Compounds 40 and 44.
Example: Methyl 3-(Hydroxy(3,4,5-trimethoxyphenyl)methyl)-

5-methoxy-1H-indole-2-carboxylate (40). A mixture of **39** (0.34 g, 0.00085 mol) and sodium borohydride (0.03 g, 0.00085 mol) in THF (2.1 mL) and water (0.12 mL) was refluxed for 2 h. After cooling, water and ethyl acetate were added. The organic layer was removed and washed with brine, dried, and filtered. Removal of the solvent gave a residue that was purified by silica gel column chromatography (ethyl acetate:*n*-hexane = 1:1 as eluent) to furnish **40** as a brown solid (0.1 g, 29%), mp 100–103 °C (from ethanol). 1H NMR ($CDCl_3$): δ 3.76 (s, 3H), 3.79 (s, 6H), 3.82 (s, 3H), 3.97 (s, 3H), 4.53 (d, $J = 1.2$ Hz, 1H), 6.50 (d, $J = 7.4$ Hz, 1H), 6.77 (s, 2H), 6.95 (d, $J = 2.4$ Hz, 1H), 7.02 (dd, $J = 6.5$ Hz, 1H), 7.28 (d, $J = 8.4$ Hz, 1H), 8.78 ppm (broad s, disappeared on treatment with D_2O , 1H). IR: ν 1707, 2937, 3322 cm^{-1} . Anal. ($C_{21}H_{23}NO_7$ (401.41)) C, H, N.

Ethyl 3-(Hydroxy(3,4,5-trimethoxyphenyl)methyl)-5-methoxy-1H-indole-2-carboxylate (44). Synthesized as **40**, starting from **43**, yield 53%, white solid, mp 115–120 °C (from ethanol). 1H NMR ($CDCl_3$): δ 1.42 (t, $J = 7.2$ Hz, 3H), 3.76 (s, 3H), 3.79 (s, 3H), 3.81 (s, 3H), 3.83 (s, 3H), 4.43 (q, $J = 6.0$ Hz, 2H), 4.44 (d, $J = 1.2$ Hz, 1H), 6.49 (d, $J = 7.2$ Hz, 1H), 6.77 (s, 2H), 6.95 (d, $J = 2.3$ Hz, 1H), 7.01 (dd, $J = 6.6$ Hz, 1H), 7.29 (d, $J = 7.3$ Hz, 1H), 8.78 ppm (broad s, disappeared on treatment with D_2O , 1H). IR: ν 1676, 3209, 3402 cm^{-1} . Anal. ($C_{22}H_{25}NO_7$ (415.44)) C, H, N.

Ethyl 5-Chloro-3-(2-oxo-2-(3,4,5-trimethoxyphenyl)acetyl)-1H-indole-2-carboxylate (22). A mixture of **21** (0.05 g, 0.00012 mol) and selenium(IV) oxide (0.05 g, 0.00045 mol) in DMSO (2 mL) was placed into the MW cavity (closed vessel mode, $P_{max} = 250$ PSI). MW irradiation of 150 W was used, the temperature being ramped from 25 to 150 °C. Once 150 °C was reached, taking about 1 min, the reaction mixture was held at this temperature for 2 min, while stirring, then cooled, diluted with water, and extracted with ethyl acetate; organic layer was washed with brine, dried, and filtered. Removal of the solvent gave a residue that was purified by silica gel column chromatography (ethyl acetate:*n*-hexane = 1:2 as eluent) to furnish **22** as a yellow solid (0.03 g, 56%), mp 177–181 °C (from ethanol). 1H NMR ($CDCl_3$): δ 1.07 (t, $J = 7.2$ Hz, 3H), 3.93 (s, 6H), 3.98 (s, 3H), 4.12 (q, $J = 7.1$ Hz, 2H), 7.35 (s, 2H), 7.42–7.43 (m, 2H), 8.40 (s, 1H), 9.50 ppm (broad s, disappeared on treatment with D_2O , 1H). IR: ν 1650, 1672, 1724, 3275 cm^{-1} . Anal. ($C_{22}H_{20}ClNO_7$ (445.85)) C, H, Cl, N.

Methyl 5-Bromo-3-(3,4,5-trimethoxyphenylthio)-1H-indole-2-carboxylate (27). A mixture of **59** (0.25 g, 0.001 mol), 3,4,5-bis(3,4,5-trimethoxyphenyl)disulfide¹⁰ (0.55 g, 0.0014 mol), and sodium hydride (0.071 g, 0.003 mol, 60% in mineral oil) in anhydrous DMF (2 mL) was placed into the MW cavity (closed vessel mode, $P_{max} = 250$ PSI). MW irradiation of 150 W was used, the temperature being ramped from 25 to 110 °C. Once 110 °C was reached, taking about 1 min, the reaction mixture was held at this temperature for 2 min, while stirring, then cooled and quenched on crushed ice and extracted with ethyl acetate. The organic layer was washed with brine, dried, and filtered. Removal of the solvent gave crude 5-bromo-3-(3,4,5-trimethoxyphenylthio)-1H-indole-2-carboxylic acid, which was used without further purification. The crude acid was dissolved in methanol (2.5 mL) and dichloromethane (10 mL) and treated with TMSDM (0.78 mL, 0.0015 mol, 2.0 M in hexane) while stirring at 25 °C for 30 min. Removal of the solvent gave a crude product that was purified by silica gel column chromatography (ethyl acetate:*n*-hexane = 1:1) to furnish **27** as a white solid (0.36 g, overall yield 79%), mp 160–162 °C (from ethanol). 1H NMR ($CDCl_3$): δ 3.72 (s, 6H), 3.81 (s, 3H), 3.98 (s, 3H), 6.48 (s, 2H), 7.33 (d, $J = 9.3$ Hz, 1H), 7.42 (dd, $J = 1.9$ and 9.3 Hz, 1H), 7.72 (d, $J = 1.9$ Hz, 1H), 9.20 ppm (broad s, disappeared on treatment with D_2O , 1H). IR: ν 1680, 3296 cm^{-1} . Anal. ($C_{19}H_{18}BrNO_5S$ (452.32)) C, H, Br, N, S.

Ethyl 5-Bromo-3-(3,4,5-trimethoxyphenylthio)-1H-indole-2-carboxylate (30). Synthesized as **27**, starting from **59** and 3,4,5-bis(3,4,5-trimethoxyphenyl)disulfide.¹⁰ The crude acid (0.5 g) was dissolved in absolute ethanol (1.7 mL) and treated with thionyl chloride (0.13 mL) at 0 °C under an Ar stream. The reaction mixture was stirred at 0 °C for 20 min, heated at 65 °C for

2 h, then cooled and diluted with water and ethyl acetate. The organic layer was removed and washed with a saturated solution of sodium hydrogen carbonate and brine, dried, and filtered. Removal of the solvent gave a crude product that was purified by silica gel column chromatography (ethyl acetate:*n*-hexane = 1:1) to give **30** as a yellow solid (0.33 g, overall yield 70%), mp 150–152 °C (from ethanol). ¹H NMR (CDCl₃): δ 1.37 (t, *J* = 7.1 Hz, 3H), 3.72 (s, 6H), 3.80 (s, 3H), 4.43 (q, *J* = 7.8 Hz, 2H), 6.48 (s, 2H), 7.33 (d, *J* = 8.7 Hz, 1H), 7.43–7.46 (m, 1H), 7.74–7.75 (m, 1H), 9.23 ppm (broad s, disappeared on treatment with D₂O, 1H). IR: ν 1672, 3299 cm⁻¹. Anal. (C₂₀H₂₀BrNO₅S (452.32)).

Methyl 5-Methoxy-3-(3,4,5-trimethoxyphenylsulfenyl)-1H-indole-2-carboxylate (37). To a cold solution of **36**¹⁰ (0.05 g, 0.00012 mol) in chloroform (5 mL) was added 3-chloroperoxybenzoic acid (0.021 g, 0.00012 mol). The reaction mixture was stirred at 25 °C for 1.5 h, then diluted with water and extracted with chloroform. The organic layer was washed with brine, dried, and filtered. Removal of the solvent gave a residue that was purified by silica gel column chromatography (ethyl acetate as eluent) to furnish **37** as a brown solid (0.05 g, yield 99%), mp 161–163 °C (from ethanol). ¹H NMR (CDCl₃): δ 3.74 (s, 3H), 3.84 (s, 9H), 3.85 (s, 3H), 6.96 (d, *J* = 9.1 Hz, 1H), 7.10 (s, 2H), 7.31 (dd, *J* = 1.9 and 9.0 Hz, 1H), 7.42 (d, *J* = 2.2 Hz, 1H), 9.37 ppm (broad s, disappeared on treatment with D₂O, 1H). IR: ν 1708, 2831, 2933 cm⁻¹. Anal. (C₂₀H₂₁NO₇S (419.45)) C, H, N, S.

Methyl 5-Methoxy-3-(3,4,5-trimethoxyphenylsulfonyl)-1H-indole-2-carboxylate (38). Was synthesized as **37**, treating **36**¹⁰ with 3-chloroperoxybenzoic acid (2 equiv), 96%, yellow solid, mp 176–180 °C (from ethanol). ¹H NMR (DMSO-*d*₆): δ 3.33 (s, 3H), 3.82 (s, 6H), 3.83 (s, 3H), 3.93 (s, 3H), 7.04 (dd, *J* = 6.5 Hz, 1H), 7.40 (s, 2H), 7.45 (d, *J* = 9.0 Hz, 1H), 7.59 (d, *J* = 2.4 Hz, 1H), 12.99 ppm (broad s, disappeared on treatment with D₂O, 1H). IR: ν 1701, 3298 cm⁻¹. Anal. (C₂₀H₂₁NO₈S (435.45)) C, H, N, S.

Ethyl 1-(3,4,5-Trimethoxybenzyl)-1H-pyrrole-2-carboxylate (46). 3,4,5-Trimethoxybenzyl chloride¹⁵ (1.083 g, 0.005 mol) was added to a well stirred mixture of ethyl 1H-pyrrole-2-carboxylate (0.63 g, 0.0045 mol), tetrabutylammonium hydrogen sulfate (1.53 g, 0.0045 mol), a 50% potassium hydroxide aqueous solution (15 mL) and dichloromethane (22 mL). The reaction mixture was stirred at 25 °C overnight, neutralized with 6 N hydrochloric acid and extracted with chloroform. The organic layer was washed with brine, dried, and filtered. Removal of the solvent gave a residue that was purified by silica gel column chromatography (dichloromethane as eluent) to furnish **46** as a yellow oil (0.64 g, 45%). ¹H NMR (CDCl₃): δ 1.21 (t, *J* = 7.1 Hz, 3H), 3.68 (s, 6H), 3.71 (s, 3H), 4.15 (q, *J* = 7.1 Hz, 2H), 5.39 (s, 2H), 6.07 (dd, *J* = 3.9 and 2.6 Hz, 1H), 6.24 (s, 2H), 6.78 (t, *J* = 2.1 Hz, 1H), 6.91 ppm (dd, *J* = 3.9 and 1.8 Hz, 1H). IR: ν 1701 cm⁻¹. Anal. (C₁₇H₂₁NO₅ (319.35)) C, H, N.

Ethyl 3,5-Dimethyl-1-(3,4,5-trimethoxybenzyl)-1H-pyrrole-2-carboxylate (47). Was synthesized as **46**, starting from ethyl 3,5-dimethyl-1H-pyrrole-2-carboxylate, yield 56%, pink solid, mp 68–70 °C (from toluene). ¹H NMR (CDCl₃): δ 1.16 (t, *J* = 7.1 Hz, 3H), 2.02 (s, 3H), 2.22 (s, 3H), 3.61 (s, 6H), 3.66 (s, 3H), 4.10 (q, *J* = 7.1 Hz, 2H), 5.37 (s, 2H), 5.71 (s, 1H), 6.03 ppm (s, 2H). IR: ν 1703 cm⁻¹. Anal. (C₁₉H₂₅NO₅ (347.41)) C, H, N.

Ethyl 3,4,5-Trimethyl-1-(3,4,5-trimethoxybenzyl)-1H-pyrrole-2-carboxylate (48). Was synthesized as **46**, starting from ethyl 3,4,5-trimethyl-1H-pyrrole-2-carboxylate, yield 45%, yellow solid, mp 82–84 °C (from ethanol). ¹H NMR (CDCl₃): δ 0.36 (t, *J* = 7.1 Hz, 3H), 1.03 (s, 3H), 1.17 (s, 3H), 1.36 (s, 3H), 2.81 (s, 6H), 2.86 (s, 3H), 3.30 (q, *J* = 7.1 Hz, 2H), 4.56 (s, 2H), 5.22 ppm (s, 2H). IR: ν 1710 cm⁻¹. Anal. (C₂₀H₂₇NO₅ (361.44)) C, H, N.

Ethyl 3,4-Diethyl-5-methyl-1-(3,4,5-trimethoxybenzyl)-1H-pyrrole-2-carboxylate (49). Was synthesized as **46**, starting from ethyl 3,4-diethyl-5-methyl-1H-pyrrole-2-carboxylate, yield 57%, yellow oil. ¹H NMR (CDCl₃): δ 0.99 (t, *J* = 7.5 Hz, 3H), 1.07 (t, *J* = 7.3 Hz, 3H), 1.21 (t, *J* = 7.1 Hz, 3H), 2.02 (s, 3H), 2.35 (q, *J* = 7.5 Hz, 2H), 2.68 (q, *J* = 7.4 Hz, 2H), 3.64 (s, 6H), 3.71 (s, 3H),

4.15 (q, *J* = 7.1 Hz, 2H), 5.44 (s, 2H), 5.96 ppm (s, 2H). IR: ν 1708 cm⁻¹. Anal. (C₂₂H₃₁NO₅ (389.49)) C, H, N.

Ethyl 1-(3,4,5-Trimethoxybenzyl)-1H-imidazole-4-carboxylate (50). A solution of DIPAD (1.29 g, 1.25 mL, 0.0064 mol) in anhydrous THF (18 mL) was added dropwise to a mixture of 3,4,5-trimethoxybenzyl alcohol (1.26 g, 0.0064 mol), ethyl 1H-imidazole-4-carboxylate²⁶ (1.0 g, 0.0071 mol), and anhydrous triphenylphosphine (1.86 g, 0.0071 mol) in the same solvent (35 mL). The reaction was stirred at 25 °C overnight under an Ar stream. The reaction mixture was concentrated in vacuo, diluted with water, and extracted with ethyl acetate. The organic layer was washed with brine, dried, and filtered. Removal of the solvent gave a residue that was purified by silica gel column chromatography (ethyl acetate:methanol = 45:5 as eluent) to furnish **50** as a colorless oil (0.2 g, 10%). ¹H NMR (CDCl₃): δ 1.26 (t, *J* = 7.4 Hz, 3H), 3.72 (s, 6H), 3.75 (s, 3H), 4.22 (q, *J* = 7.1 Hz, 2H), 5.36 (s, 2H), 6.33 (s, 2H), 7.54 (s, 1H), 7.69 ppm (s, 1H). IR: ν 1695 cm⁻¹. Anal. (C₁₆H₂₀N₂O₅ (320.34)) C, H, N.

Ethyl 1-(3,4,5-Trimethoxybenzoyl)-1H-pyrrole-2-carboxylate (51). To a stirred mixture of potassium *tert*-butoxide (0.26 g, 0.0023 mol) and 18-crown-6 (0.47 g, 0.0018 mol) in anhydrous THF (25 mL) was added dropwise a solution of ethyl 1H-pyrrole-2-carboxylate (0.25 g, 0.0018 mol) in the same solvent (25 mL). After cooling to 0 °C for 15 min, a solution of 3,4,5-trimethoxybenzoyl chloride (0.41 g, 0.0018 mol) in the same solvent (25 mL) was added dropwise. The reaction mixture was stirred at 25 °C for 4 h and then concentrated to a small volume and extracted with ethyl acetate. The organic layer was washed with brine, dried, and filtered. Removal of the solvent gave a residue that was purified by silica gel column chromatography (dichloromethane as eluent) to furnish **51** as an orange oil (0.05 g, 8%). ¹H NMR (CDCl₃): δ 1.09 (t, *J* = 7.1 Hz, 3H), 3.78 (s, 6H), 3.82 (s, 3H), 4.02 (q, *J* = 7.1 Hz, 2H), 6.24 (m, 1H), 6.94 (s, 2H), 6.99 (m, 1H), 7.18 ppm (m, 1H). IR: ν 1670, 1703 cm⁻¹. Anal. (C₁₇H₁₉NO₆ (333.34)) C, H, N.

Ethyl 1-(3,4,5-Trimethoxybenzoyl)-1H-imidazole-4-carboxylate (52) and Ethyl 1-(3,4,5-Trimethoxybenzoyl)-1H-imidazole-5-carboxylate (53). To a solution of ethyl imidazole 4-carboxylate²⁶ (0.5 g, 0.0035 mol) in anhydrous dichloromethane (10 mL) was added dropwise a solution of 3,4,5-trimethoxybenzoyl chloride (0.41 g, 0.0018 mol) in the same solvent (10 mL). The reaction mixture was refluxed for 2.5 h and, after cooling, quenched on crushed ice. The organic layer was removed and washed with brine, dried, and filtered. Removal of the solvent gave a residue that was purified by silica gel column chromatography (ethyl acetate as eluent). The initial eluate furnished **52** as a white solid (0.17 g, 15%), mp 130–133 °C (from ethanol). ¹H NMR (CDCl₃): δ 1.34 (t, *J* = 7.1 Hz, 3H), 3.84 (s, 6H), 3.90 (s, 3H), 4.34 (q, *J* = 7.1 Hz, 2H), 6.96 (s, 2H), 8.06 (s, 1H), 8.09 ppm (s, 1H). IR: ν 1672, 1702 cm⁻¹. Anal. (C₁₆H₁₈N₂O₆ (334.32)) C, H, N. Further elution with the same solvent afforded **53** as a white solid (0.12 g, 13%), mp 140–143 °C (from ethanol). ¹H NMR (CDCl₃): δ 1.40 (t, *J* = 7.1 Hz, 3H), 3.90 (s, 6H), 3.97 (s, 3H), 4.40 (q, *J* = 7.1 Hz, 2H), 7.02 (s, 2H), 8.16 ppm (s, 2H). IR: ν 1674, 1707 cm⁻¹. Anal. (C₁₆H₁₈N₂O₆ (334.32)) C, H, N.

1-(3,4,5-Trimethoxybenzyl)-1H-pyrrole-2-carboxylic acid (54). A mixture of **46** (0.23 g, 0.00072 mol) and potassium hydroxide (0.12 g, 0.0022 mol) in methanol:water (1:1) (10 mL) was refluxed for 3 h. After cooling, the reaction mixture was washed with dichloromethane; the aqueous layer was made acidic with 2 N hydrochloric acid (pH = 2) and extracted with dichloromethane. The organic layer was washed with water, dried, filtered, and evaporated to give **54** as a brown solid (0.15 g, 74%), mp 80–81 °C (from ethanol). ¹H NMR (CDCl₃): δ 3.68 (s, 6H), 3.71 (s, 3H), 5.36 (s, 2H), 6.12 (dd, *J* = 3.85 and 2.6 Hz, 1H), 6.27 (s, 2H), 6.85 (t, *J* = 2.0 Hz, 1H), 7.04 (dd, *J* = 3.9 and 1.7 Hz, 1H), 10.69 ppm (broad s, disappeared on treatment with D₂O, 1H). IR: ν 1703, 2995 cm⁻¹. Anal. (C₁₅H₁₇NO₅ (291.30)) C, H, N.

2-(2-Hydroxyethoxy)ethyl 3,4,5-Trimethyl-1-(3,4,5-trimethoxybenzyl)-1H-pyrrole-2-carboxylate (55). A mixture of **48**

(0.05 g, 0.0014 mol) and potassium hydroxide (0.043 g, 0.00077 mol) in diethylene glycol (1 mL) was heated at 140 °C for 3 h. After cooling, water and ethyl acetate were added and the layers separated. The organic layer was washed with brine, dried, and filtered. Removal of the solvent gave a residue that was purified by silica gel column chromatography (ethyl acetate as eluent) to give **55** as a yellow oil (0.02 g, 34%). ¹H NMR (CDCl₃): δ 1.89 (s, 3H), 2.02 (s, 3H), 2.23 (s, 3H), 3.50 (m, 2H), 3.62 (m, 2H), 3.66 (m, 3H), 3.68 (s, 6H), 3.73 (s, 3H), 4.28 (m, 2H), 5.41 (s, 2H), 6.06 ppm (s, 2H). IR: ν 1705, 2836 cm⁻¹. Anal. (C₂₂H₃₁NO₇ (421.28)) C, H, N.

1-(3,4,5-Trimethoxybenzyl)-1H-imidazole-4-carboxylic Acid Hydrochloride (56). A mixture of **50** (0.08 g, 0.00025 mol) and 37% hydrochloric acid (1.5 mL) was refluxed for 1.5 h. After cooling, the reaction mixture was washed with ethyl acetate. The aqueous layer was evaporated in vacuo. The residue was dissolved in 2-propanol (1.5 mL) and cooled to -78 °C. Upon addition of *n*-hexane, the suspension was filtered to give **56** as a white solid (0.05 g, 68%), mp 163–166 °C (from methanol). ¹H NMR (CD₃OD): δ 3.77 (s, 3H), 3.85 (s, 6H), 5.73 (s, 2H), 6.82 (s, 2H), 8.24 (s, 1H), 9.22 (s, 1H), 12.10 (broad s, disappeared on treatment with D₂O, 1H). IR: ν 1705, 3100 cm⁻¹. Anal. (C₁₄H₁₆N₂O₅·HCl (328.75)) C, H, Cl, N.

Ethyl 2-(2-(4-Bromophenyl)hydrazono)propanoate (57). A mixture of 4-bromophenylhydrazine hydrochloride (5.7 g, 0.0255 mol), ethyl pyruvate (2 g, 1.91 mL, 0.017 mol), and sodium acetate (2.79 g, 0.034 mol) in ethanol (40 mL) was placed into the MW cavity (open vessel mode). MW irradiation at 250 W was used, the temperature being ramped from 25 to 100 °C. Once 100 °C was reached, taking about 2 min, the reaction mixture was held at this temperature for 5 min while stirring. The reaction mixture was cooled at 0 °C, with stirring, and filtered to give **57**, yield 90%, mp 142–144 °C (from ethanol). ¹H NMR (CDCl₃): δ 1.39 (t, *J* = 7.2 Hz, 3H), 2.12 (s, 3H), 4.33 (q, *J* = 7.1 Hz, 2H), 7.10 (d, *J* = 6.7 Hz, 2H), 7.40 (d, *J* = 6.9 Hz, 2H), 7.64 ppm (broad s, disappeared on treatment with D₂O, 1H). IR: ν 1576, 1675, 3290 cm⁻¹. Anal. (C₁₁H₁₃BrN₂O₂ (285.14)).

Ethyl 5-Bromo-1H-indole-2-carboxylate (58). Compound **57** (35.15 g, 0.123 mol) was added in portions to PPA (350 g) preheated at 110 °C. The mixture was stirred at the same temperature for 30 min and then quenched with ice–water. The solid was filtered, washed with water, dried, and recrystallized from ethanol to give **58** as a brown solid (32.95 g, 60%), mp 160–161 °C. ¹H NMR (CDCl₃): δ 1.43 (t, *J* = 7.1 Hz, 3H), 4.43 (q, *J* = 7.1 Hz, 2H), 7.15–7.16 (m, 1H), 7.31 (d, *J* = 8.1 Hz, 1H), 7.41 (dd, *J* = 7.0 Hz, 1H), 7.84 (m, 1H), 9.98 ppm (broad s, disappeared on treatment with D₂O, 1H). IR: ν 1690, 3311 cm⁻¹. Anal. (C₁₁H₁₀BrNO₂ (268.11)).

5-Bromo-1H-indole-2-carboxylic Acid (59). A mixture of **58** (0.25 g, 0.001 mol) in 3 N sodium hydroxide (2 mL) was placed into the MW cavity (closed vessel mode, *P*_{max} = 250 PSI). MW irradiation at 150 W was used, the temperature being ramped from 25 to 110 °C. Once 110 °C was reached, taking about 1 min, the reaction mixture was held at this temperature for 2 min while stirring. After cooling, the reaction mixture was made acidic with 3 N hydrochloric acid (pH = 2) and extracted with ethyl acetate; the organic layer was washed with brine, dried, filtered, and evaporated to give **59** as a brown solid (0.23 g, 95%), mp 188 °C (from ethanol). ¹H NMR (DMSO-*d*₆): δ 7.05 (s, 1H), 7.32 (dd, *J* = 8.9 Hz, 1H), 7.39 (d, *J* = 8.8 Hz, 1H), 7.85 (d, *J* = 2.1 Hz, 1H), 11.94 (broad s, disappeared on treatment with D₂O, 1H), 12.61 ppm (broad s, disappeared on treatment with D₂O, 1H). IR: ν 1652, 2850, 3422 cm⁻¹. Anal. (C₉H₆BrNO₂ (240.05)).

Methyl 5-Bromo-1H-indole-2-carboxylate (60). To a cold suspension of **59** (3.4 g, 0.014 mol) in anhydrous methanol (13.4 mL) was added thionyl chloride (1.6 mL) dropwise. The reaction mixture was stirred at the same temperature for 20 min and then heated at 65 °C for 2 h under an Ar stream, then cooled and diluted with water and ethyl acetate. The layers

were separated, and the organic phase was washed with a saturated solution of sodium hydrogen carbonate and brine, dried, filtered, and evaporated to give **60** as a white solid (3.43 g, 96%), mp 217–220 °C (from ethanol/cyclohexane), lit.²⁵ 211.8–213.6.

2-(3,4,5-Trimethoxyphenyl)acetyl Chloride. This compound was synthesized by treating a cold solution of 3,4,5-trimethoxyphenylacetic acid (0.25 g, 0.0011 mol) in anhydrous THF (5 mL) with oxalyl chloride (0.28 g, 0.19 mL, 0.0022 mol). Immediately afterward, a catalytic amount (2 drops) of anhydrous DMF was added, and vigorous bubbling ensued. After 10 min, the reaction mixture was carefully concentrated in vacuo to provide a viscous oil. Fresh anhydrous THF was added, and the solution was concentrated in vacuo again to furnish 2-(3,4,5-trimethoxyphenyl)acetyl chloride (0.27 g, yellow oil), which was used without further purification.

Molecular Modeling. All molecular modeling studies were performed on a MacPro dual 2.66 GHz Xeon running Ubuntu 8. The tubulin structure was downloaded from the PDB (<http://www.rcsb.org/>; PDB code 1SA0).³ Hydrogen atoms were added to the protein, using Molecular Operating Environment (MOE) 2007.09,²⁷ and minimized, keeping all the heavy atoms fixed until a rmsd gradient of 0.05 kcal mol⁻¹ Å⁻¹ was reached. Ligand structures were built with MOE and minimized using the MM-FF94x forcefield until a rmsd gradient of 0.05 kcal mol⁻¹ Å⁻¹ was reached. The docking simulations were performed using FlexX²⁸ with the MOE interface. The rmsd of the trimethoxyphenyl moiety for each of the compounds evaluated was calculated in comparison with ring A of DAMA-colchicine, and the results from the docking were scored using this value.²⁹ The images presented here were created with Zodiack.³⁰

Biology. Tubulin Assembly. The reaction mixtures contained 0.8 M monosodium glutamate (pH 6.6 with hydrochloric acid in 2 M stock solution), 10 μM tubulin, and varying concentrations of drug. Following a 15 min preincubation at 30 °C, samples were chilled on ice, GTP to 0.4 mM was added, and turbidity development was followed at 350 nm in a temperature controlled recording spectrophotometer for 20 min at 30 °C. Extent of reaction was measured. Full experimental details were previously reported.³¹

[³H]Colchicine Binding Assay. The reaction mixtures contained 1.0 μM tubulin, 5.0 μM [³H]colchicine, and 5.0 μM inhibitor and were incubated 10 min at 37 °C. Complete details were described previously.³²

Cell Lines. Methodology for the evaluation of the growth of human MCF-7 breast carcinoma cells was previously described.³² Human HeLa cells (from carcinoma of the uterine cervix) and HCT116/chr3 cells (from colon carcinoma) were grown at 37 °C in a humidified atmosphere containing 5% carbon dioxide in D-MEM (Gibco BRL, UK) supplemented with 10% fetal calf serum, 4 mM glutamine, 2 mM sodium pyruvate, 100 U/mL penicillin, and 0.1 mg/mL streptomycin (all reagents were from Celbio, Italy). For the HCT116/chr3 cells, the medium also included 500 μg/mL of the selection compound G418 (Gibco). Cells were trypsinized when subconfluent and seeded in T75 flasks at a concentration of 10⁵/mL. U937 (human monocytic leukemia cell line) and J774.1 cells (murine macrophage cell line) were cultured in RPMI 1640 medium containing 10% fetal calf serum, 50 μg/mL each of penicillin and streptomycin, and 2 mM glutamine. Human melanoma M14 cells and human embryonic kidney (HEK) 293 cells were grown at 37 °C in Dulbecco's modified Eagle's medium containing 10 mM glucose (DMEM-HG) supplemented with 10% fetal calf serum and 50 μg/mL each of penicillin and streptomycin.

The *P. tridactylis* PtK2 cells, the A10 rat embryonic aortic smooth muscle cells, the human umbilical vein endothelial cells, and the human aortic smooth muscle cells were obtained from the American Type Tissue Collection and grown as recommended by the supplier, except that a 5% CO₂ atmosphere was used with all cells.

Morphological Analysis. Cells grown in T75 flasks and treated with 100 μM **24** for 24 h were observed with an Olympus IX71 microscope and photographed with a Cool SNAPES_{ES} Photo-metric digital camera.

Cell Viability Assay. HeLa and HCT116/chr3 cells. Cells were seeded in 96-well plates at a density of 1×10^3 cells/100 μL well. Twenty-four hours later, cells were treated with the test compound (stock solution: 10 mM in DMSO, kept at room temperature in the dark) used at increasing concentrations (0.1–100 μM) for 24 h. Cells were harvested at the end of the treatment or washed with phosphate-buffered saline and incubated in drug-free medium for an additional 24 h. To rule out a possible effect of the solvent, parallel samples were incubated in complete medium containing 1% DMSO. At the end of the treatments, 20 μL of CellTiter96 Aqueous One Solution Reagent (Promega) was added to each well. The plates were then incubated for 4 h at 37 °C and analyzed with a microplate reader (Gio. De Vita, Roma, Italy) at 492 nm. Experiments were performed in quadruplicate and repeated three times.

M14, HEK, U937, and J774.1 cells. Cell viability was determined using the 3-[4,5-dimethylthiazol-2,5-diphenyl-2H-tetrazolium bromide (MTT) colorimetric assay. The test is based on the ability of mitochondrial dehydrogenase to convert, in viable cells, the yellow MTT reagent into a soluble blue formazan dye. Cells were seeded into 96-well plates to a density of 10^5 cells/100 μL well. After 24 h of growth to allow attachment to the wells, compounds were added at various concentrations (10, 30, 50, 100, 150, and 200 nM). After 24 or 48 h of growth and after removal of the culture medium, 100 μL /well of medium containing 1 mg/mL of MTT was added. Cell cultures were further incubated at 37 °C for 2 h in the dark. The MTT solution was then removed, and 100 μL DMSO was added to dissolve formazan crystals. Absorbance at 550 nm was measured using a plate reader. Experiments were performed in triplicate. As a control, 0.5% DMSO was added to untreated cells.

Time-Lapse Microscopy. Effect of drug treatment on HEK and M14 cell morphology was determined by TLM using a Leica CTR6500 microscope. Images were captured every hour for a 48 h period. Plates (96-well) were incubated under standard culture conditions and kept at 37 °C in a 5% carbon dioxide atmosphere for the observation period (up to 48 h).

Yeast. *S. cerevisiae* yeast wild type strain BY4741 (*Mat a his3 Δ 1 leu2 Δ 0 met15 Δ 0 ura3 Δ 0*) was used. Cells were grown at 28 °C in minimal medium (0.67% yeast nitrogen base without amino acids) containing 2% glucose (synthetic dextrose, SD) supplemented with 20 $\mu\text{g}/\mu\text{L}$ of the appropriate nutritional supplements. A fresh exponential culture (5×10^6 cells/mL) of the yeast were incubated for 18 h at 28 °C with the compound of interest at 20 μM . The cells were then centrifuged for 5 min at 13000g at 4 °C, washed twice with distilled water, and resuspended in SD (1 mL). Cell suspensions (15 μL) were transferred in 60 μL of fresh SD medium, serially diluted 10-fold, incubated overnight at 28 °C, and spotted onto YP plates (1% yeast extract, 2% peptone) supplemented with 2% glucose (YPD). The plates were incubated at 28 °C for three days before recording cell growth.

Acknowledgment. This research was funded in part by Istituto Pasteur—Fondazione Cenci Bolognietti, and Progetti di Ricerca di Università, Sapienza Università di Roma. A.C. thanks Istituto Pasteur—Fondazione Cenci Bolognietti for his Borsa di Studio per Ricerche all'Estero. G.L.R. was supported by a fellowship from FIRC. L.M. thanks Progetti di Ricerca di Università, Sapienza Università di Roma, for her Contratto di Collaborazione Esterna per Progetti di Ricerca (Bando 2/2007, Dipartimento di Studi Farmaceutici). This research was also partially supported by a grant of the Fondazione Banca del Monte di Lombardia (Pavia, Italy)

to A.I.S. V.G. is a Ph.D. student from the University of Pavia (Dottorato in Scienze biomolecolari e biotecnologie).

Supporting Information Available: Effects of compounds **24**, **27–29**, **36**, **39**, and **41** on murine macrophage J774.1 cell morphology. Elemental analyses of new derivatives **7**, **8**, **10**, **11**, **13**, **14**, **16**, **17**, **19–23**, **25–32**, **35**, **37–41**, and **43–56**. This material is available free of charge via the Internet at <http://pubs.acs.org>.

References

- (1) Teicher, B. A. Newer cytotoxic agents: attacking cancer broadly. *Clin. Cancer Res.* **2008**, *14*, 1610–1617.
- (2) Bhattacharyya, B.; Panda, D.; Gupta, S.; Banerjee, M. Antimitotic activity of colchicine and the structural basis for its interaction with tubulin. *Med. Res. Rev.* **2008**, *28*, 155–183.
- (3) Ravelli, R. B.; Gigant, B.; Curmi, P. A.; Jourdain, I.; Lachkar, S.; Sobel, A.; Knossow, M. Insight into tubulin regulation from a complex with colchicine and a stathmin-like domain. *Nature* **2004**, *428*, 198–202.
- (4) Nogales, E.; Whittaker, M.; Milligan, R. A.; Downing, K. H. High-resolution model of the microtubule. *Cell* **1999**, *96*, 79–88.
- (5) Nettles, J. H.; Li, H.; Cornett, B.; Krahn, J. M.; Snyder, J. P.; Downing, K. H. The binding mode of epothilone A on α , β -tubulin by electron crystallography. *Science* **2004**, *305*, 866–869.
- (6) Buey, R. M.; Calvo, E.; Barasoain, I.; Pineda, O.; Edler, M. C.; Matesanz, R.; Cerezo, G.; Vanderwal, C. D.; Day, B. W.; Sorensen, E. J.; Lopez, J. A.; Andreu, J. M.; Hamel, E.; Diaz, J. F. Cyclo-treptin binds covalently to microtubule pores and luminal taxoid binding sites. *Nat. Chem. Biol.* **2007**, *3*, 117–125.
- (7) Lin, M. C.; Ho, H. H.; Pettit, G. R.; Hamel, E. Antimitotic natural products combretastatin A-4 and combretastatin A-2: studies on the mechanism of their inhibition of the binding to colchicine to tubulin. *Biochemistry* **1989**, *28*, 6984–6991.
- (8) Beckers, T.; Mahboobi, S. Natural, semisynthetic and synthetic microtubule inhibitors for cancer therapy. *Drugs Future* **2003**, *28*, 767–785.
- (9) Sridhare, M.; Macapinlac, M. J.; Goel, S.; Verdier-Pinard, D.; Fojo, T.; Rothenberg, M.; Colevas, D. The clinical development of new mitotic inhibitors that stabilize the microtubule. *Anticancer Drugs* **2004**, *15*, 553–555.
- (10) De Martino, G.; La Regina, G.; Coluccia, A.; Edler, M. C.; Barbera, M. C.; Brancale, A.; Wilcox, E.; Hamel, E.; Artico, M.; Silvestri, R. Arylthioindoles, potent inhibitors of tubulin polymerization. *J. Med. Chem.* **2004**, *47*, 6120–6123.
- (11) De Martino, G.; Edler, M. C.; La Regina, G.; Coluccia, A.; Barbera, M. C.; Barrow, D.; Nicholson, R. I.; Chiosis, G.; Brancale, A.; Hamel, E.; Artico, M.; Silvestri, R. Arylthioindoles, potent inhibitors of tubulin polymerization. 2. Structure–activity relationships and molecular modeling studies. *J. Med. Chem.* **2006**, *49*, 947–954.
- (12) La Regina, G.; Edler, M. C.; Brancale, A.; Kandil, S.; Coluccia, A.; Piscitelli, F.; Hamel, E.; De Martino, G.; Matesanz, R.; Díaz, J. F.; Scovassi, A. I.; Prosperi, E.; Lavecchia, A.; Novellino, E.; Artico, M.; Silvestri, R. New arylthioindoles inhibitors of tubulin polymerization. 3. Biological evaluation, SAR and molecular modeling studies. *J. Med. Chem.* **2007**, *50*, 2865–2874.
- (13) Tron, G. C.; Pirali, T.; Sorba, G.; Pagliai, F.; Busacca, S.; Genazzani, A. A. Medicinal chemistry of combretastatin A4: present and future directions. *J. Med. Chem.* **2006**, *49*, 1–12.
- (14) Liou, J.-P.; Chang, Y.-L.; Kuo, F.-M.; Chang, C.-W.; Tseng, H.-Y.; Wang, C.-C.; Yang, Y.-N.; Chang, J.-Y.; Lee, S.-J.; Hsieh, H.-P. Concise synthesis and structure–activity relationships of combretastatin A-4 analogues, 1-arylthioindoles, and 3-arylthioindoles as novel classes of potent antitubulin agents. *J. Med. Chem.* **2004**, *47*, 4247–4257.
- (15) Mori, K.; Takaishi, H. Synthetic microbial chemistry. XXII. Synthesis of monocerin, an antifungal, insecticidal and phytotoxic heptaketide metabolite of *Exserohilum monoceras*. *Tetrahedron* **1989**, *45*, 1639–1646.
- (16) Mitsunobu, O.; Yamada, M. Preparation of esters of carboxylic and phosphoric acid via quaternary phosphonium salts. *Bull. Chem. Soc. Jpn.* **1967**, *40*, 2380–2382.
- (17) Botstein, D.; Chervitz, S. A.; Cherry, J. M. Yeast as a model organism. *Science* **1997**, *277*, 1259–1260.
- (18) Almeida, B.; Silva, A.; Mesquita, A.; Sampaio-Marques, B.; Rodrigues, F.; Ludovico, P. Drug-induced apoptosis in yeast. *Biochim. Biophys. Acta* **2008**, *1783*, 1436–1448.

- (19) Zabrocki, P.; Bastiaens, I.; Delay, C.; Bammens, T.; Ghillebert, R.; Pellens, K.; De Virgilio, C.; Van Leuven, F.; Winderick, J. Phosphorylation, lipid raft interaction and traffic of alpha-synuclein in a yeast model for Parkinson's disease. *Biochim. Biophys. Acta* **2008**, *1783*, 1767–1780.
- (20) Cassidy-Stone, A.; Chipuk, J. E.; Ingerman, E.; Song, C.; Yoo, C.; Kuwana, T.; Kurth, M. J.; Shaw, J. T.; Hinshaw, J. E.; Green, D. R.; Nunnari, J. Chemical inhibition of the mitochondrial division dynamin reveals its role in Bax/Bak-dependent mitochondrial outer membrane permeabilization. *Dev. Cell* **2008**, *14*, 193–204.
- (21) Nguyen, T. L.; McGrath, C.; Hermone, A. R.; Burnett, J. C.; Zaharevitz, D. W.; Day, B. W.; Wipf, P.; Hamel, E.; Gussio, R. A common pharmacophore for a diverse set of colchicine site inhibitors using a structure-based approach. *J. Med. Chem.* **2005**, *48*, 6107–6116.
- (22) Dupeyre, G.; Chabot, G. G.; Thoret, S.; Cachet, X.; Seguin, J.; Guenard, D.; Tillequin, F.; Scherman, D.; Koch, M.; Michel, S. Synthesis and biological evaluation of (3,4,5-trimethoxyphenyl)indol-3-ylmethane derivatives as potential antivasular agents. *Bioorg. Med. Chem.* **2006**, *14*, 4410–4426.
- (23) Liou, J.-P.; Wu, C.-Y.; Hsieh, H.-P.; Chang, C.-Y.; Chen, C.-M.; Kuo, C.-C.; Chang, J.-Y. 4- and 5-Aroylindoles as novel classes of potent antitubulin agents. *J. Med. Chem.* **2007**, *50*, 4548–4552.
- (24) Jia, Y.; Zhu, J. Palladium-catalyzed, modular synthesis of highly functionalized indoles and tryptophans by direct annulation of substituted *o*-haloanilines and aldehydes. *J. Org. Chem.* **2006**, *71*, 7826–7834.
- (25) Tullberg, E.; Schacher, F.; Peters, D.; Frejd, T. Solvent-free Heck–Jeffery reactions under ball-milling conditions applied to the synthesis of unnatural amino acids precursors and indoles. *Synthesis* **2006**, *7*, 1183–1189.
- (26) Davis, D. P.; Kirk, K. L.; Cohen, L. A. New synthesis of 2-nitroimidazoles. *J. Heterocycl. Chem.* **1982**, *19*, 253–256.
- (27) Molecular Operating Environment (MOE 2007.09). Chemical Computing Group, Inc. Montreal, Quebec, Canada, <http://www.chemcomp.com>.
- (28) FlexX 3.0; BioSolveIT GmbH; Sankt Augustin, Germany; <http://www.biosolveit.de>. Accessed on 11/12/2008.
- (29) Code “fragment_rmsd.svl” obtained from SVL exchange website: *SVL Exchange: An SVL Code Exchange Site for the MOE User Community*; Chemical Computing Group, Inc.: Montreal, Canada, 2004; <http://svl.chemcomp.com>. Accessed on 11/12/2008.
- (30) Zodiac 0.5b; <http://www.zeden.org>. Accessed on 11/12/2008.
- (31) Hamel, E. Evaluation of antimitotic agents by quantitative comparisons of their effects on the polymerization of purified tubulin. *Cell Biochem. Biophys.* **2003**, *38*, 1–21.
- (32) Verdier-Pinard, P.; Lai, J.-Y.; Yoo, H.-D.; Yu, J.; Marquez, B.; Nagle, D. G.; Nambu, M.; White, J. D.; Falck, J. R.; Gerwick, W. H.; Day, B. W.; Hamel, E. Structure–activity analysis of the interaction of curacin A, the potent colchicine site antimitotic agent, with tubulin and effects of analogs on the growth of MCF-7 breast cancer cells. *Mol. Pharmacol.* **1998**, *53*, 62–76.